



Review

# Calmodulin-Cork Model of Gap Junction Channel Gating—One Molecule, Two Mechanisms

Camillo Peracchia 

Department of Pharmacology and Physiology, School of Medicine and Dentistry, University Rochester, Rochester, NY 14642, USA; camillo.peracchia@gmail.com

Received: 18 June 2020; Accepted: 10 July 2020; Published: 13 July 2020



**Abstract:** The Calmodulin-Cork gating model is based on evidence for the direct role of calmodulin (CaM) in channel gating. Indeed, chemical gating of cell-to-cell channels is sensitive to nanomolar cytosolic calcium concentrations  $[Ca^{2+}]_i$ . Calmodulin inhibitors and inhibition of CaM expression prevent chemical gating. CaMCC, a CaM mutant with higher  $Ca^{2+}$ -sensitivity greatly increases chemical gating sensitivity (in CaMCC the  $NH_2$ -terminal EF-hand pair (res. 9–76) is replaced by the COOH-terminal pair (res. 82–148). Calmodulin colocalizes with connexins. Connexins have high-affinity CaM binding sites. Several connexin mutants paired to wild-type connexins have a high gating sensitivity that is eliminated by inhibition of CaM expression. Repeated transjunctional voltage ( $V_j$ ) pulses slowly and progressively close a large number of channels by the chemical/slow gate (CaM lobe). At the single-channel level, the chemical/slow gate closes and opens slowly with on-off fluctuations. The model proposes two types of CaM-driven gating: “Ca-CaM-Cork” and “CaM-Cork”. In the first, gating involves  $Ca^{2+}$ -induced CaM-activation. In the second, gating takes place without  $[Ca^{2+}]_i$  rise. The Ca-CaM-Cork gating is only reversed by a return of  $[Ca^{2+}]_i$  to resting values, while the CaM-Cork gating is reversed by  $V_j$  positive at the gated side.

**Keywords:** gap junctions; connexins; channel gating; calcium; calmodulin; cell communication; cell-to-cell channels; cell coupling; cell uncoupling

## 1. Introduction

In most tissues, cells in contact with each other exchange cytosolic molecules of low molecular weight via channels aggregated at gap junctions. Gap junction mediated cell-to-cell communication allows neighboring cells to coordinate and regulate many functional activities in mature and developing organs [1–3]. A gap junction channel is made of the interaction of two hemichannels (connexons/innexons) that form a hydrophilic pathway across the two apposed plasma membranes and the extracellular space (gap). Each connexon/innexon is an oligomer of six proteins (connexins/innexins) that span the plasma membrane and create a hydrophilic pore insulated from lipid bilayer and extracellular medium.

Gap junction channels have been thought to possess as many as four types of gates: fast transjunctional voltage ( $V_j$ ) gate, slow  $V_j$ -gate, chemical gate and gate sensitive to membrane potential ( $V_m$ ). However, since the behavior of the slow  $V_j$ -gate and the  $V_m$ -sensitive is the same as that of the chemical gate, most likely these gates are the same. We have named this gate “chemical/slow gate” [1].

In 2000, we proposed a calmodulin (CaM)-mediated “cork-type” gating model [4]. The model proposes two mechanisms. One, “Ca-CaM-Cork”, envisions physical blockage of the channel’s mouth by a CaM lobe (N-lobe?), likely to be combined with conformational connexin changes induced by  $Ca^{2+}$ -CaM binding to connexin sites. The other, “CaM-Cork”, also proposes a physical blockage of the channel’s mouth by a CaM lobe, but without  $Ca^{2+}$ -activation. The first is only reversed by the return

of intracellular  $\text{Ca}^{2+}$  concentration ( $[\text{Ca}^{2+}]_i$ ) to resting values. The latter is reversed by  $V_j$  positive at the gated side.

## 2. Why Calmodulin?

### 2.1. Gating is Activated by Nanomolar Calcium Concentrations $[\text{Ca}^{2+}]_i$

Numerous studies have demonstrated that  $[\text{Ca}^{2+}]_i$  in the high nanomolar range are effective on channel gating in many vertebrate and invertebrate cells. They include: cardiomyocytes [5–7], crayfish axons [8,9], *Xenopus laevis* oocytes [10], rat lacrimal epithelial cells [11], Novikoff hepatoma cells [12,13], astrocytes [14–16], lens-cultured cells [17], human fibroblasts [18], cultured cells expressing Cx43 [19], pancreatic cells [20–25] and neuro-2a cells (N2a) expressing Cx43, among others.

Much of our work on chemical gating has tested cell uncoupling resulting from cytosolic acidification. Since low  $\text{pH}_i$  had been reported to cause chemical gating by acting directly on the channel's gates [26], starting in 1990 we questioned extensively whether the  $\text{H}^+_i$  effect is direct or mediated by an increase in  $[\text{Ca}^{2+}]_i$ . Our data, obtained in a variety of vertebrate [10,12] and invertebrate [8,9,27] cells, have convinced us that cytosolic acidification does not directly affect the channel gates, but rather its effect is mediated by  $\text{Ca}^{2+}_i$ ; rev. in [1,28]. In fact, most relevant in this respect are our findings in Novikoff hepatoma cells, in which  $\text{pH}_i = 6.1$  does not affect gating as long as  $[\text{Ca}^{2+}]_i$  is buffered to low nanomolar concentrations by 1,2-bis(*o*-aminophenoxy) ethane-*N,N,N',N'*-tetraacetic acid) (BAPTA) added to the patch-pipette solutions [12].

Based on gating sensitivity to nanomolar  $[\text{Ca}^{2+}]_i$ , it is reasonable to believe not only that  $\text{Ca}^{2+}_i$  is a fine modulator of cell-to-cell communication, but also that a  $\text{Ca}^{2+}$ -modulated protein, CaM being the most likely, mediates the  $\text{Ca}^{2+}_i$ -induced channel gating. Direct action of  $\text{Ca}^{2+}_i$  is very unlikely because the cytosolic domains of connexins do not contain high-affinity  $\text{Ca}^{2+}$ -binding sites. In contrast, they do have high-affinity CaM binding sites [1] (see in the following).

### 2.2. CaM Inhibitors Prevent Chemical Gating

Several decades ago, we first proposed the role of CaM in gap junction channel gating based on evidence that CaM inhibitors prevent chemical uncoupling of *Xenopus* embryonic cells [29–31]. Over the years, various CaM inhibitors have been reported to be effective in inhibiting chemical gating. They include: trifluoperazine (TFP) [30,31], calmidazolium (CDZ) [19,29,32] and N-(6-aminoethyl)-5-chloro-1-naphthalenesulfonamide hydrochloride (W7) [32–36].

### 2.3. Inhibition of CaM Expression Prevents Chemical Gating

Inhibition of CaM expression by injection of oligonucleotides antisense to the two CaM mRNAs expressed in oocytes results in progressive loss of uncoupling efficiency in oocytes expressing the native connexin Cx38 [10], Cx32-mutants [37] or Cx45 channels [38]. Chemical gating efficiency partially recovers with CaM injection [10].

### 2.4. A CaM Mutant with Higher $\text{Ca}^{2+}$ -Sensitivity Greatly Enhances Gating Sensitivity

In 2000, we tested the CaM role in gating in *Xenopus* oocytes overexpressing the CaM mutant CaMCC (Figure 1) [39,40] by measuring junctional conductance ( $G_j$ ). For measuring  $G_j$ , a transjunctional voltage ( $V_j$ ) gradient is created by imposing a voltage pulse ( $V_1$ ) to one oocyte (oocyte 1) while maintaining  $V_2$  at membrane potential ( $V_m$ ); thus,  $V_j = V_1$ . The negative-feedback current ( $I_2$ ), injected by the clamp amplifier in oocyte 2 for maintaining  $V_2$  constant at  $V_m$ , is used for calculating  $G_j$ , as it is identical in magnitude to the junctional current ( $I_j$ ), but of opposite sign ( $I_j = -I_2$ );  $G_j = I_j/V_j$  (Ohm's law). In CaMCC, the CaM's  $\text{NH}_2$ -terminal EF-hand pair (res. 9–76) is replaced by the COOH-terminal pair (res. 82–148; Figure 1A). Since the  $\text{Ca}^{2+}$ -affinity of the carboxy-terminal EF-hand pair is greater than that of the  $\text{NH}_2$ -terminal pair by approximately one order of magnitude [41], we thought that CaMCC expression might increase the sensitivity of chemical gating.

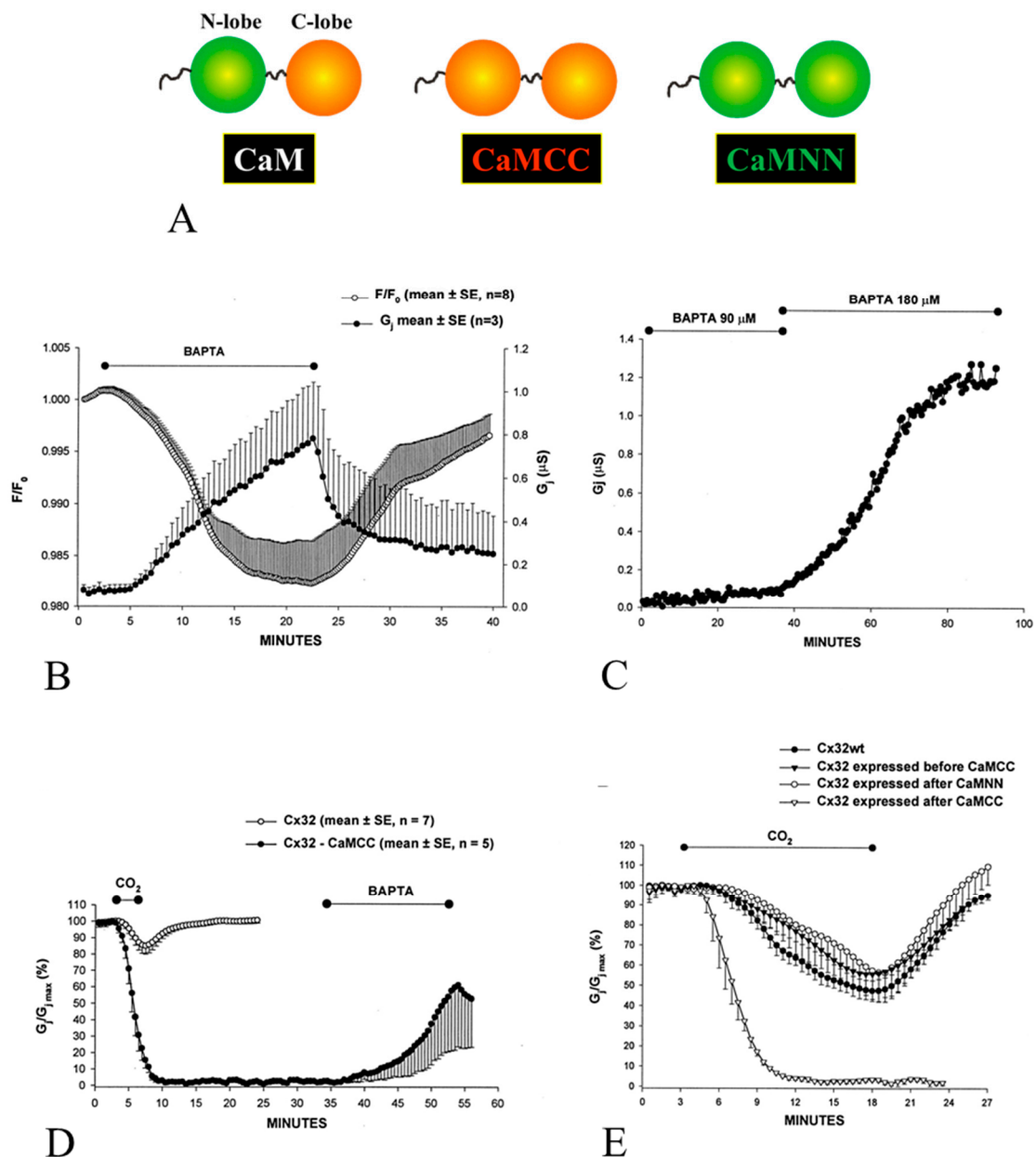


**Figure 1.** In oocytes expressing CaMCC (A) before Cx32,  $G_j$  is very low (B), but rapidly increases with 180  $\mu$ M BAPTA superfusion (B,C) as  $[Ca^{2+}]_i$ , measured with Calcium Green-1, drops (B, F/F<sub>0</sub>). In CaMCC the NH<sub>2</sub>-terminal EF-hand pair (res. 9–76) is replaced by the COOH-terminal pair (res. 82–148). Lower [BAPTA] (90  $\mu$ M) are much less effective (C). Cx32 channels expressed after CaMCC are more sensitive to 100% CO<sub>2</sub> than controls (D,E), as  $G_j$  rapidly drops to zero (D,E) with CO<sub>2</sub> applications for as short as 3 min (D) or 15 min (E; mean  $\pm$  standard error, SE,  $n = 3$ ), while in controls it decreases by only  $\sim$ 15% even with CO<sub>2</sub> applications as long as 15 min (E; mean  $\pm$  SE,  $n = 7$ ). After CO<sub>2</sub> washout,  $G_j/G_{jmax}$  remains at 0% but rapidly increases with 180  $\mu$ M BAPTA superfusion (D). Expression of Cx32 before CaMCC (E; mean  $\pm$  SE,  $n = 3$ ) or expression of CaMNN (A) has no effect on gating (E; mean  $\pm$  SE,  $n = 3$ ). From [39].

In fact, in oocytes expressing CaMCC and Cx32  $G_j$  was minimal, but substantially increased when  $[Ca^{2+}]_i$ , monitored with Calcium Green-1, was lowered by 180  $\mu$ M BAPTA superfusion (Figure 1B,C). Indeed, CaMCC enhances Ca<sup>2+</sup>-gating-sensitivity so much that gating is even activated by resting  $[Ca^{2+}]_i$ . Significantly, the effect of CaMCC is only observed when its expression precedes that of Cx32, which indicates that it successfully competes with CaM wild-type for Cx32 interaction. In contrast,

the mutant CaMNN, in which the NH<sub>2</sub>-terminal pair replaces the COOH-terminal pair had no effect (Figure 1E), suggesting that CaMNN does not effectively compete against wild-type CaM for Cx32 interaction. The significance of the CaMCC/Cx32 sequence of expression indicates that CaMCC, as native CaM, interacts with Cx32 before connexon assembly.

The enhanced gating sensitivity induced by CaMCC's expression was further confirmed by testing the effect of 100% carbon dioxide (CO<sub>2</sub>), which causes a drop in pHi to ~6.3 and results in an increase in [Ca<sup>2+</sup>]<sub>i</sub>. In the presence of CO<sub>2</sub>, G<sub>j</sub> rapidly dropped to zero, while in controls it only decreased by ~15% (Figure 1D). With CO<sub>2</sub> washout, G<sub>j</sub> remained at zero indefinitely, but begun recovering (reversibly) with 180 μM BAPTA superfusion (Figure 1D), which obviously decreased [Ca<sup>2+</sup>]<sub>i</sub> below resting values.

The same result was obtained in oocytes expressing Cx43 or COOH-terminus (CT) deleted Cx43 (Cx43-TR257) after CaMCC expression (Figure 2)—note that these Cx43 data are new and not published elsewhere. Note that CT-deleted Cx43 (Cx43-TR257) has been reported to be relatively insensitive to 100% CO<sub>2</sub> [42–44], which prompted the creation of the ball-and-chain model, which envisions a particle-receptor interaction in which the CT domain acts as a gating particle by binding to a separate region of the connexin. [43]. In contrast, Figure 2A,B demonstrates that Cx43's CT domain is not needed for chemical gating, as also reported by Wei and coworkers [45]. As with Cx32 channels (Figure 1D), in some experiments, Cx43-TR257 channels expressed after CaMCC remained indefinitely uncoupled following CO<sub>2</sub> washout (Figure 2C,D), but G<sub>j</sub> reversibly recovered with 180 μM BAPTA (Figure 2C,D) as it did with Cx32 channels (Figure 1D).

Two phenomena are notable with Cx43-TR257 in the presence and absence of CaMCC:

1. With 3 min CO<sub>2</sub> application, in Cx43-TR257 channels, the G<sub>j</sub> time-course is monophasic, as paradoxically G<sub>j</sub> just increases (Figure 2A). In contrast, with CaMCC the G<sub>j</sub> change is biphasic, as G<sub>j</sub> drops to ~50% following a brief rise (Figure 2A).
2. With 15 min CO<sub>2</sub> application, in Cx43-TR257 channels, the G<sub>j</sub> time-course is biphasic both in the presence and absence of CaMCC, as it rises before dropping (Figure 2B).

Significantly, this biphasic time-course (Figure 2B) is also observed often in different wild-type connexin channels. An example is provided by Cx45 channels (Figure 3) [38]. We have suggested that the early G<sub>j</sub> rise may result from activation of the Ca/CaM-Kinase II (CaMKII) cascade [38], which is known to increase G<sub>j</sub> [46,47] and open Cx43 hemichannels [48]. If this were the case, a likely scenario could be that with CO<sub>2</sub> application an early, moderate, [Ca<sup>2+</sup>]<sub>i</sub> rise (↑[Ca<sup>2+</sup>]<sub>i</sub>; Figure 2A,B and Figure 3) opens a number of dormant channels, likely to be in closed state via the CaM-Cork mechanism (see in the following) (Figure 2A,B, and Figure 3), perhaps via activation of the CaMKII cascade. In contrast, the subsequent, larger [Ca<sup>2+</sup>]<sub>i</sub> rise (↑↑[Ca<sup>2+</sup>]<sub>i</sub>; Figure 2A,B and Figure 3) would close the channels by direct Ca<sup>2+</sup>-CaM interaction (Ca-CaM-Cork gating; see in the following) (Figures 2 and 3). The reason why we believe that the early G<sub>j</sub> rise of Cx43 channels results from moderate [Ca<sup>2+</sup>]<sub>i</sub> rise is that with brief (3 min) exposure to CO<sub>2</sub> the G<sub>j</sub> curve is just monophasic (Figure 2A; yellow circles). This may suggest that a moderate [Ca<sup>2+</sup>]<sub>i</sub> may activate the CaMKII cascade, but is not enough to activate the Ca-CaM-Cork gating mechanism. In our Ca-Cork model, the gating element is suggested to be the CaM's N-lobe, which has a lower Ca-sensitivity than the C-lobe. This could be the reason why the CaMKII cascade is activated a lower [Ca<sup>2+</sup>]<sub>i</sub> than the CaM's N-lobe.

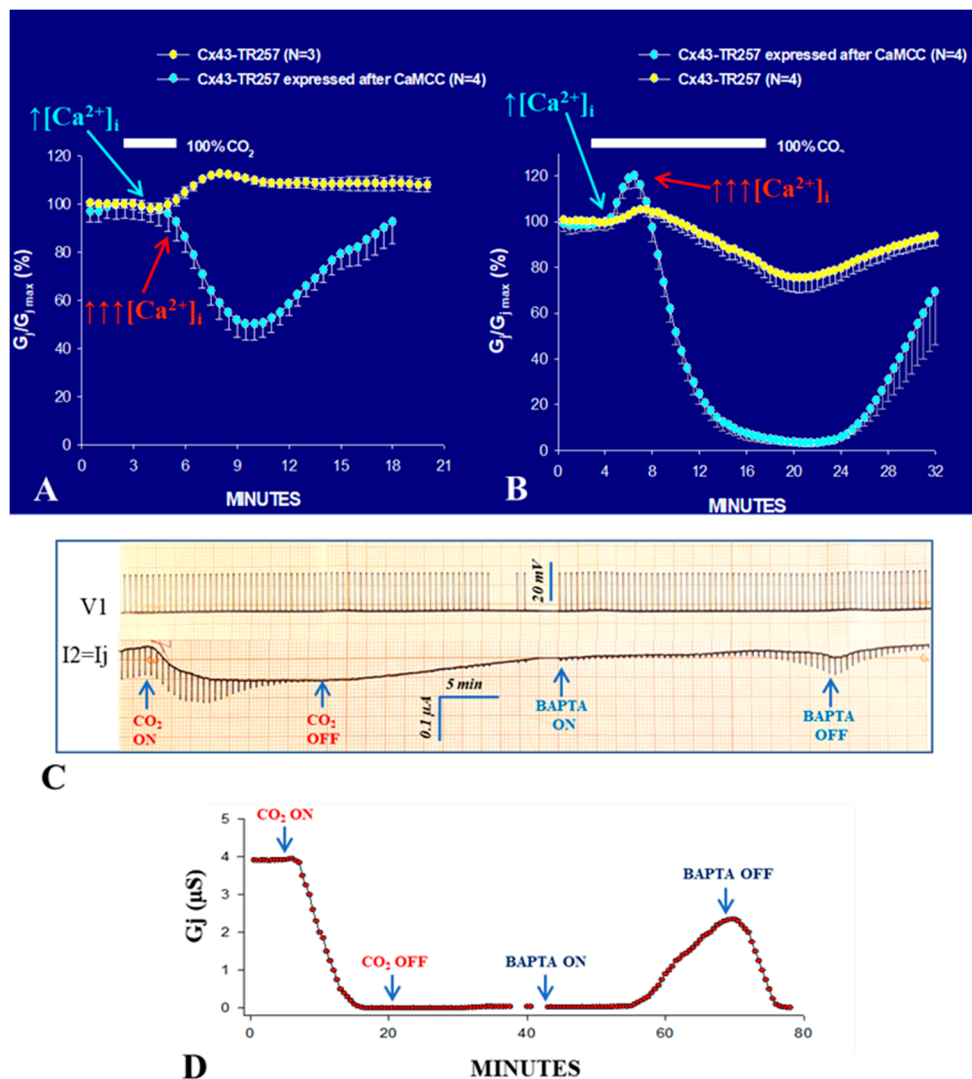


**Figure 2.** CT-deleted Cx43 channels (Cx43TR257), expressed after CaMCC, are much more sensitive to CO<sub>2</sub> than controls (A and B), as G<sub>j</sub> rapidly drops to ~50% (A) and nearly 0% (B) with 3 and 15 min 100% CO<sub>2</sub> applications, respectively, while in controls G<sub>j</sub> decreases by only ~25% even with 15 min CO<sub>2</sub> (B). Curiously, in controls paradoxically G<sub>j</sub> increases reversibly with brief applications of CO<sub>2</sub> (A); similarly, G<sub>j</sub> increases before dropping in control Cx43TR257 (B). The initial G<sub>j</sub> rise may result from activation of the CaMKII cascade (see text). After CO<sub>2</sub>-washout, in some experiments, G<sub>j</sub> remains indefinitely at nearly 0% (C,D), but reversibly increases with 180 μM BAPTA superfusion (C,D). An original voltage (V1 = V<sub>j</sub>) and current (I2 = I<sub>j</sub>) chart record is shown in C. The changes in G<sub>j</sub> (μS) of the experiment shown in C are shown in D (G<sub>j</sub> = I<sub>j</sub>/V<sub>j</sub>). These Cx43 data are mine, new and not published elsewhere.

Evidence that both phenomena are eliminated by inhibition of CaM expression (Figure 3) confirms the CaM-participation in this phenomenon. Although there is no evidence that CaMKII directly phosphorylates Cx45 channels, it is known that it phosphorylates Cx43/CT serine residues [49]. While in Cx43TR257 most of the serine residues of CT [49] are lost, three of them (S244, S255 and S257) are preserved. The loss of CO<sub>2</sub>-induced G<sub>j</sub> rise with inhibition of CaM expression suggests that with CaM inhibition, unlike in controls, most of the channels are in an open state. It is likely that the reduced CaM concentration prevents some channels from being closed by the CaM-Cork gating mechanism at rest.

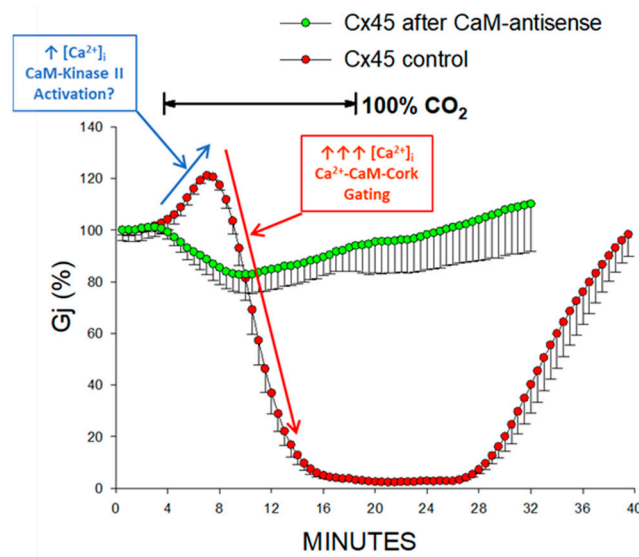


**Figure 3.** The junctional conductance ( $G_j$ ), monitored in *Xenopus* oocyte pair expressing Cx45 during  $\text{CO}_2$  application, has a biphasic course: initial rise followed by a rapid drop to full uncoupling (red circles). Since activation of CaMKII increases  $G_j$  (see text), the initial  $G_j$  rise may result from activation of the CaMKII cascade and opening of dormant, CaM-Cork gated channels. We believe that subsequent rapid  $G_j$  drop results from the activation of the Ca-CaM-Cork mechanism. Inhibition of CaM expression greatly reduces the  $\text{CO}_2$  sensitivity, as  $G_j$  reversibly drops (monophasically) by only ~17% (green circles)—the absence of  $G_j$  rise suggests that with reducing  $[\text{CaM}]_i$  at rest, most channels are open. From [38].

### 2.5. Colocalization of CaM and Connexins

Calmodulin–connexin interaction was tested by immunofluorescence microscopy [39,40]. In HeLa cells expressing Cx32, CaM and Cx32 colocalize at cell–cell contact as well as in few cytoplasmic spots (Figure 4) [39,40]. Similar data were obtained with Cx43 and Cx37 (Sotkis and Peracchia, unpublished data), and with Cx50 [50,51] and Cx36 [52].

The CaM-Cx32 colocalization was further proven by confocal fluorescence microscopy in HeLa cells expressing Cx32 linked to the green fluorescent protein (Cx32-GFP) and CaM linked to the red fluorescent protein (CaM-RFP) [1,40,53]. In these cells, however, CaM and Cx32 only colocalized in the cytoplasm, as these cells did not form gap junctions, probably because steric hindrance prevented connexin oligomerization into connexons [40,53].

Recently, direct visualization of CaM-Cx45 interaction was reported in live cells by Bioluminescence Resonance Energy Transfer (BRET) [54]; the CaM-Cx45 interaction was  $\text{Ca}^{2+}$ -dependent and was prevented by W7. The interaction involved the CaM-binding site in the second half of the cytoplasmic loop (CL2, res. 164–186; Figure 5). This was confirmed by the high-affinity binding of fluorescence-labeled CaM to a peptide matching the CL2 domain [54]. In fact, there is evidence for  $\text{Ca}^{2+}$ -dependent and independent CaM-binding to the CL2 sequence of Cx45 [55,56]. The  $\text{Ca}^{2+}$ -independent CaM-CL2 binding confirms earlier evidence that CaM is linked to connexins at resting  $[\text{Ca}^{2+}]_i$  (~50 nM) [37,39,40,53,54,56].

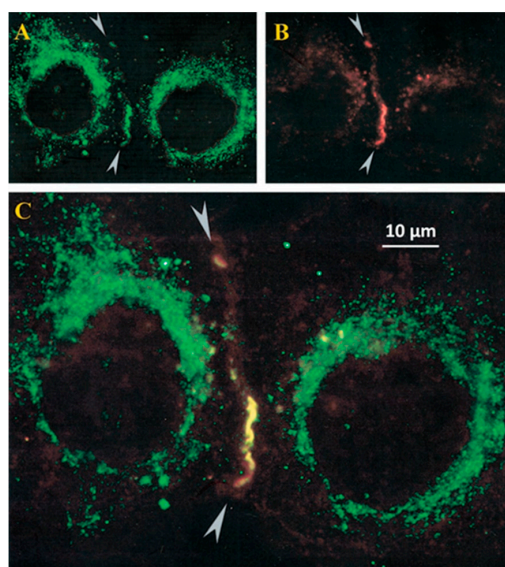


**Figure 4.** Immunofluorescence labeling of CaM (A) and Cx32 (B) in HeLa cells expressing Cx32. CaM and Cx32 colocalize in linear (regions between arrowheads) and punctated areas of cell–cell contact (C). Labeling is also seen in the cytoplasm (A–C); this is likely to correspond to CaM and CaM linked to Cx32 in cytoplasmic organelles. Scale bar 10  $\mu\text{m}$ . From [39].

#### 2.6. Connexins Have High-Affinity CaM Binding Sites

Calmodulin binding sites were first identified in 1988 in Cx32: one at NH<sub>2</sub>-terminus (NT) and one at the initial domain of the COOH-terminus (CT1) [57] (Figure 5A). Their binding to CaM was proven by several studies [58–60]. CaM also binds to CT1 of Cx43 [61], Cx35 and Cx34.7 [52,62] and Cx36 [52]. However, the CT1 site is unlikely to be relevant for chemical gating because neither Cx32's CT deletion by 84% [63,64] nor Cx43's CT deletion at res. 257 affects chemical gating efficiency [45]. In contrast, CL2 (Figure 5A) is likely to be most relevant to chemical gating [65,66] (Figure 5B,C).

We first focused on the CL2 domain in 1996, when we tested in oocytes the CO<sub>2</sub> sensitivity of channels formed by Cx32 and Cx38 chimeras and mutants. As mentioned earlier, Cx32 and Cx38 make channels with opposite CO<sub>2</sub> gating sensitivity (Figure 6B) [65,66]. Channels made of Cx32/38CL (Figure 6A; Cx38's CL replaced by that of Cx32) reproduced almost perfectly Cx38 channel gating in magnitude and time course (Figure 6B) [66]. For identifying more precisely the most relevant CL domain, we expressed Cx32/Cx38 chimeras in which either the 1st half (CL1) or the 2nd half of Cx38's CL replaced that of Cx32(CL2)(Figure 6A) [65]. Cx32/Cx38CL2 channels (Cx32 with Cx38's CL2) were like Cx38 channels in terms of CO<sub>2</sub> sensitivity, but G<sub>j</sub> recovered faster (Figure 6B). Significantly, they matched Cx32 channels in fast-V<sub>j</sub> gating sensitivity [65]. The data indicate that CL1 and CL2 contain domains relevant to fast-V<sub>j</sub>- and chemical-gating, respectively [65]. This is consistent with evidence that CL2 contains a CaM binding site (Figure 5B,C) [1].

For testing the gating efficiency of channels made of Cx43 mutants that lack the CL2's CaM-binding site, Zhou and coworkers expressed in HeLa cells two mutants linked to EYFP (a fluorescent protein) [67]. The lack of the site abolished Ca<sup>2+</sup>-dependent gating, confirming that CL2 contains the CaM-binding domain relevant to chemical gating [67]. The importance of this site was further confirmed with Cx43 [19], Cx50 [68], or Cx44 [69,70] channels.

A study tested by small-angle X-ray scattering a synthetic peptide matching the CL2's CaM-binding domain of Cx43 (res. 144–158), in order to detect potential Ca<sup>2+</sup>-induced conformational changes [71]. With peptide interaction, CaM assumed a more globular conformation, suggesting that CaM binds to the peptide in typical “collapsed” conformation [71].

Xu and coworkers [19] reported that ionomycin application increases [Ca<sup>2+</sup>]<sub>i</sub> and causes G<sub>j</sub> to drop by 95% in N2a cells expressing human Cx43, but not in cells expressing human Cx40. This at first



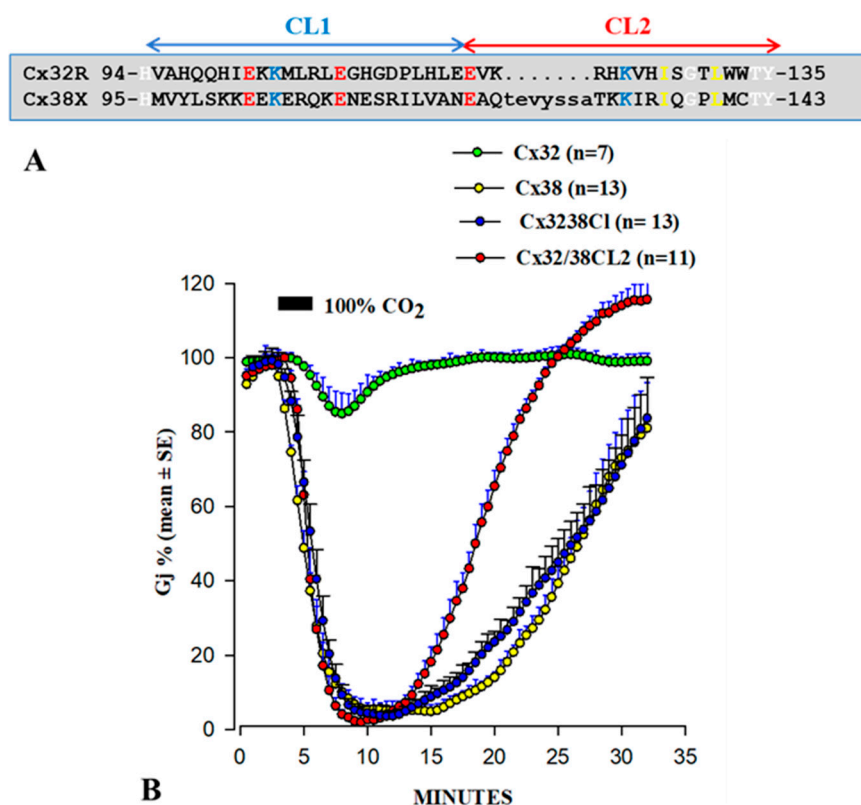


**Figure 6.** Sequences of the cytoplasmic loop (CL) of rat Cx32 and *Xenopus* Cx38 (A). G<sub>j</sub> changes induced by 100% CO<sub>2</sub>, monitored in oocytes expressing Cx32, Cx38, or Cx32/38 chimeras are shown in B. Channels made of Cx32/38CL (Cx32's CL being replaced by that of Cx38) or Cx32/38CL2 (Cx32's CL2 being replaced by that of Cx38) reproduce precisely the gating efficiency of Cx38 channels in both magnitude and rate (B), but G<sub>j</sub> recovers faster in Cx32/38CL2 channels. Note that CL2 contains a CaM-binding site (see Figure 5A,B). Adapted from [65,66].

### 2.7. CaM Is Linked to Connexins at Resting [Ca<sup>2+</sup>]<sub>i</sub>

There are reasons to believe that CaM is linked to connexins at resting [Ca<sup>2+</sup>]<sub>i</sub> as well. There is evidence that CaMCC overexpression greatly decreases the V<sub>j</sub> sensitivity of Cx32 channels [39]. Furthermore, the V<sub>j</sub> sensitivity of Cx45 channels is significantly inhibited by blocking CaM expression [38]—note that Cx45 channels are quite sensitive to V<sub>j</sub> and the chemical/slow gate mediates V<sub>j</sub> gating [74]. The behavior of mutant/Cx32 channels also indicates that CaM is linked to connexins at resting [Ca<sup>2+</sup>]<sub>i</sub> (~50 nM), because inhibition of CaM expression in mutant/Cx32 channels greatly decreases the effectiveness of V<sub>j</sub> on G<sub>j</sub> [37]. Even more relevant is immunofluorescent evidence that CaM colocalizes with connexins at gap junctions of the cultured cell at resting [Ca<sup>2+</sup>]<sub>i</sub> (Figure 4) [39,40].

Evidence that CaM is linked to connexins at resting [Ca<sup>2+</sup>]<sub>i</sub> has been recently confirmed by an *in vitro* study that tested CaM-binding to peptides matching the CL2's CaM binding site of Cx32, Cx35, Cx45 and Cx57, with and without Ca<sup>2+</sup> [55,56]. Fluorescence changes of the double-labeled FRET (Föster Resonance Energy Transfer) probe and Ca<sup>2+</sup>-sensitive TA-CaM (2-chloro-(epsilon-amino-Lys75)-[6-[4-(N,N-diethylamino)phenyl]-1,3,5-triazin-4-yl]calmodulin) were revealed by fluorescence spectroscopy and stopped-flow fluorimetry [75] at physiological ionic strength (pH 7.5, 20 °C). The following kD values were obtained (Table 1):

**Table 1.** CaM binding to CL2.

Connexins	kD (With Ca <sup>2+</sup> )	kD (Without Ca <sup>2+</sup> )
Cx32	40 ± 4 nM	280 ± 10 nM
Cx35	31 ± 2 nM	2,67 ± 0.09 μM
Cx45	75 ± 4 nM	78 ± 1 nM
Cx57	60 ± 6 nM	32 ± 14 nM

### 2.8. Potential Role of CaM-Activated Enzymes in Chemical Gating?

The possibility that CaM induces channel gating via enzyme activation, was tested with inhibitors and/or activators of many enzymes [53]. However, none of them affected G<sub>j</sub> and/or gating efficiency [53]. The potential role of Ca<sup>2+</sup>-proteases is also unlikely because proteolysis would be irreversible, while the recovery rate of Ca<sup>2+</sup>-induced uncoupling is much faster than the turnover-time of connexins' (half-life = ~3 h) [76].

## 3. Why Cork?

### 3.1. Behavior of Heterotypic Mutant-Wildtype Channels

We first proposed the “cork” gating hypothesis based on the unusual behavior of certain Cx32 mutants heterotypically paired with Cx32 wild-type [4,37,77] (Figures 7 and 8).

Since the behavior of these heterotypic channels is qualitatively the same, we will focus here just on channels made of Cx32 tandems paired with Cx32 wild-type (tandem-32); a tandem is a dimer in which two Cx32 monomers are concatenated NT-to-CT (Figure 7A). Tandem-32 channels displayed a unique I<sub>j</sub>-V<sub>j</sub> behavior (Figure 7B,D). With tandem side negative, as V<sub>j</sub> was increased stepwise from 20 to 120 mV initial and final I<sub>j</sub> progressively decreased to very low values and the channels were sensitive to even the lowest V<sub>j</sub> values (−20 mV). With tandem side positive, I<sub>j</sub> gradually increased to high values and up to V<sub>j</sub> = 80mV I<sub>j</sub> monitored at the end of the pulse was higher than initial I<sub>j</sub> (Figure 7D). This V<sub>j</sub> behavior indicates that V<sub>j</sub> positive at mutant gradually renders operational more channels. Significantly, this asymmetric behavior is absent following inhibition of CaM expression (Figure 7E) [37].

To test the idea that V<sub>j</sub> positive at the tandem side renders operational a greater number of channels, the effect of applying repeated long 60 mV V<sub>j</sub> pulses (tandem side positive) was tested (Figure 7C). The following I<sub>j</sub> behaviors were observed: monophasic I<sub>j</sub> rise (pulses 1–3); biphasic I<sub>j</sub> time-course (pulses 4–9), displaying an initial gradual I<sub>j</sub> rise followed by exponential I<sub>j</sub> decay; and ultimately a fairly conventional I<sub>j</sub> behavior (pulses 10–18). The application of conventional V<sub>j</sub> protocols (tandem side positive), after the train of V<sub>j</sub> pulses, resulted in an I<sub>j</sub> behavior similar to that of homotypic Cx32 channels (Figure 7C; pulses 19–27). This clearly suggested that V<sub>j</sub> positive at mutant side renders progressively operational numerous previously “dormant” (gated) channels.

To determine the time-course of the G<sub>j</sub> changes in response to positive and negative V<sub>j</sub> at the tandem side, tandem-32 channels were subjected to long, steady-state, V<sub>j</sub> gradients [77] (Figure 8A,B). In oocytes initially clamped at V<sub>m</sub> = −20 mV (V<sub>j</sub> = 0), 40–80 mV steady-state V<sub>j</sub> gradients (tandem side positive) slowly and exponentially increased G<sub>j</sub> (τ = ~1 min) by as much as 400% (Figure 8A,B). In contrast, steady-state V<sub>j</sub> gradients negative at the tandem side reduce G<sub>j</sub> by over 85% (Figure 8A,B). Upon returning to V<sub>j</sub> = 0 from V<sub>j</sub> = 40 mV (tandem side positive), G<sub>j</sub> suddenly increased before dropping (Figure 7A,B). This was caused by the reopening of fast V<sub>j</sub>-gates at the Cx32 side (Cx32 is a negative gater). As predicted, this did not occur when V<sub>j</sub> polarity was switched from positive to negative (Figure 8B), as in this case while fast V<sub>j</sub>-gates open at the Cx32wt's side (positive V<sub>j</sub> side) fast V<sub>j</sub>-gates close at the tandem side (negative V<sub>j</sub> side).

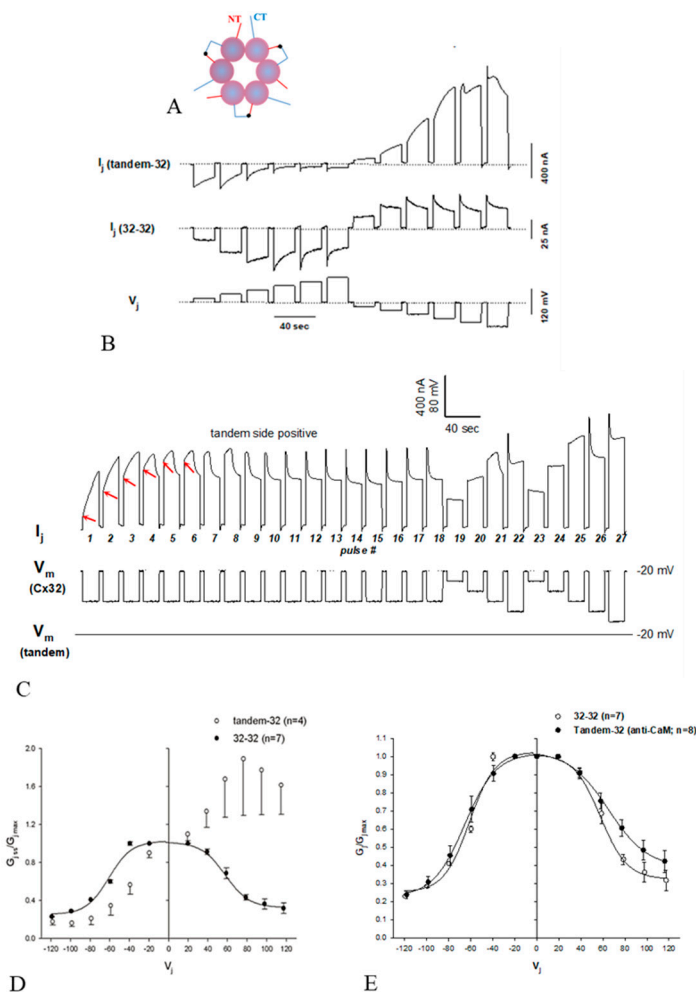


**Figure 7.**  $I_j/V_j$  records of *Xenopus* oocyte pairs expressing either homotypic Cx32 channels (32–32) or heterotypic tandem-32 channels (A,B). While 32–32 channels manifest a characteristic  $I_j$  sensitivity to  $V_j$  (B), tandem-32 channels show an unusual behavior (B). With mutant side negative (B, left), initial and final  $I_j$  gradually drop to very low values, while with mutant side positive (B, right),  $I_j$  gradually increases to high values and only at  $V_j = 100$ – $120$  mV, a more typical  $I_j$  behavior appears. With repeated application of 60-mV  $V_j$  pulses (tandem side positive), 3 types of  $I_j$  behavior are observed: monophasic  $I_j$  increase (C, pulses 1–3), biphasic  $I_j$  time-course (C, pulses 4–9) and conventional  $I_j$  behavior (C, pulses 10–18). Subsequent applications of the  $V_j$  protocol (tandem side positive) result in fairly normal  $I_j$  behaviors (C, pulses 19–27). The asymmetric  $I_j$ - $V_j$  behavior of tandem-32 channels is demonstrated in plots of normalized  $G_j$  versus  $V_j$  (D). Significantly, the asymmetrical  $I_j/V_j$  behavior is not observed following inhibition of CaM expression (E). (B,C) from [77]; (D,E) from [37].

The slow change in  $G_j$  is clearly consistent with the gating behavior of the chemical/slow gate, which is clearly different from the behavior of the fast  $V_j$ -gate. There are many reasons for this distinction [77], one is that in all connexins tested the chemical/slow gate closes at the negative  $V_j$  side, whereas the fast  $V_j$ -gate closes at the negative or positive  $V_j$  side depending on the connexin type. In fact, heterotypic channels (4pos/E-26) between Cx26 and a Cx26 mutant (4pos/E), in which four basic CT residues are mutated to acidic residues (E), behave qualitatively as heterotypic tandem-32 (or 5R/E-32) channels when subjected to  $V_j$  gradients (Figure 9) [53]. This is important because the fast  $V_j$ -gates of Cx26 and Cx32 are activated by opposite  $V_j$  polarities—Cx32 is a “negative gater” while Cx26 is a “positive gater” [78]. This obviously suggests that in Cx32 and Cx26 mutant channels this gating behavior results from the activity of the negatively charged chemical/slow gate (CaM’s N-lobe?). Significantly, the asymmetrical  $V_j$  behavior of heterotypic mutant-Cx32 channels disappeared with

inhibition of CaM expression (Figure 7E) [37]. Based on these data and single-channel records (see in the following), we proposed the “CaM-Cork” gating model [4] (see in the following).

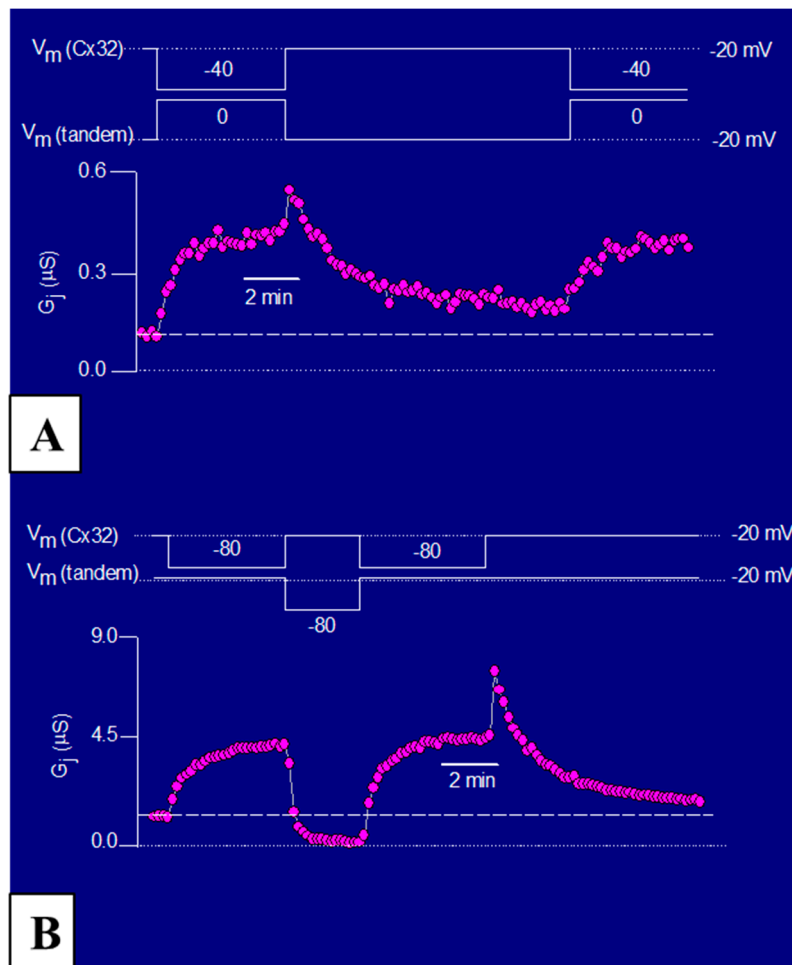
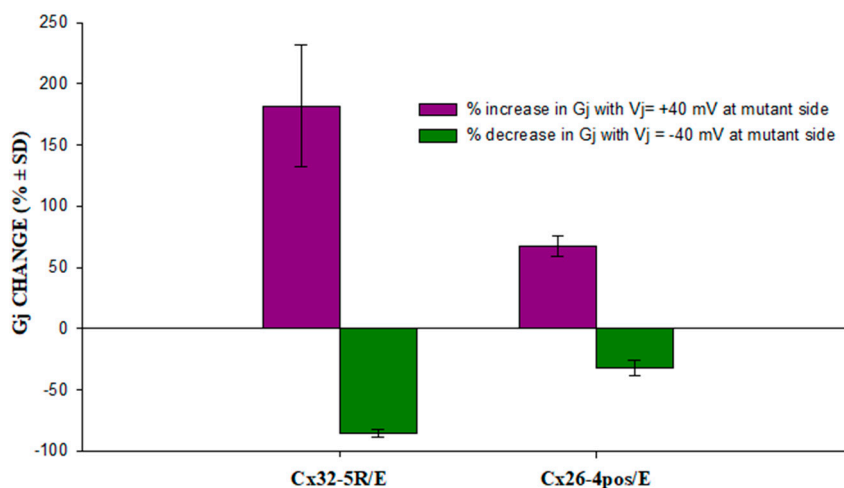


**Figure 8.** Response of  $G_j$  to steady-state  $V_j$  in tandem-32 channels (A,B). In oocytes initially clamped at  $V_m = 20$  mV ( $V_j = 0$ ), a 40–60 mV  $V_j$  step (tandem side positive) exponentially increases  $G_j$  in tandem-32 channels (A,B). Upon return to  $V_j = 0$  mV from  $V_j = 40$  mV (A),  $G_j$  decreases exponentially to near control values. With  $V_j$  reversal to 60 mV (tandem side negative),  $G_j$  decreases exponentially below control values (B), indicating that  $V_j$  negative at the tandem side actively closes channels. Upon return to  $V_j = 0$  from  $V_j = 40$  (A) or 60 (B) mV (tandem side positive),  $G_j$  increases abruptly before dropping (A,B), because the fast  $V_j$ -gates of the Cx32 side reopen (Cx32 is a negative gater). Of course, this is not observed with  $V_j$  polarity reversal (B) because while the fast  $V_j$ -gates open at Cx32wt side (positive  $V_j$  side) they close at the tandem side (negative  $V_j$  side). From [77].



**MUTANTS OF Cx32 AND Cx26 TESTED HETEROLOGICALLY AGAINST WILD-TYPE Cx32 AND Cx26, RESPECTIVELY**

Cx32 mutant 5R/E: R215E, R219E, R220E, R223E, R224E  
 Cx26 mutant 4pos/E: R215E, K220E, K222E, R223E

**Figure 9.** Percent G<sub>j</sub> change in oocytes expressing Cx32-mutant (Cx32-5R/E) or Cx26-mutant (Cx26/4pos-E) heterotypic channels. Cx26-4pos/E channels behaved as Cx32-5R/E (or tandem-32) channels when subjected to V<sub>j</sub> gradients, in spite of the fact that their fast V<sub>j</sub> gates are activated by opposite V<sub>j</sub> polarities (Cx32 is “negative gater”, Cx26 is “positive gater”). This confirms that the slow G<sub>j</sub> change with V<sub>j</sub> gradients is a gating behavior based on the activity of the chemical/slow gate, which is clearly distinct from that of the fast V<sub>j</sub> gate[1]. Adapted from [1].

### 3.2. Chemical/Slow Gating Behavior at the Single-Channel Level

The behavior of the chemical/slow gate was studied by a double whole-cell clamp (DWCC) at minimal G<sub>j</sub> values in rat fibroblasts and Cx43-expressing HeLa cells during exposure to 100% CO<sub>2</sub> [79]. We recorded junctional current (I<sub>j</sub>), single-channel conductance (γ<sub>j</sub>) and I<sub>j</sub>-kinetics, during uncoupling and recoupling at three V<sub>j</sub> gradients (Figure 10). Since the fast V<sub>j</sub>-gate is only activated by V<sub>j</sub> gradients >40–50 mV, by monitoring gating at three V<sub>j</sub> gradients: V<sub>j</sub> = 30 mV (fast V<sub>j</sub>-gate open; Figure 10A), V<sub>j</sub> = 55 mV (fast V<sub>j</sub>-gate flickering; Figure 10B) or V<sub>j</sub> = 70 mV (fast V<sub>j</sub>-gate mostly closed), we were able to study in detail the individual behavior of the chemical/slow gate and the fast V<sub>j</sub> gate.

With V<sub>j</sub> = 30 mV, CO<sub>2</sub> just caused slow I<sub>j</sub> transitions from open to closed channel states (transition time = ~10 ms; chemical/slow gating activity; Figure 10A). With V<sub>j</sub> = 55 mV, we monitored fast I<sub>j</sub> flickering between open (γ<sub>j</sub> main state) and residual (γ<sub>j</sub> residual) states (transition time = ~2 ms; fast V<sub>j</sub> gate activity) and slow I<sub>j</sub> transitions between open and closed channel states (chemical/slow gate activity; Figure 10B). With V<sub>j</sub> = 70 mV, aside from slow I<sub>j</sub> transitions between open and closed channel states, CO<sub>2</sub> caused slow transitions between residual and closed channel states (chemical/slow gate activity) [79].

During recoupling, the channels reopened, a slow transition (transition time = ~10 ms) from closed to open state (chemical/slow gate activity; Figure 10A,B), was followed by fast I<sub>j</sub> flickering between open and residual state (fast V<sub>j</sub> gate activity; Figure 10B). These data agree with earlier reports on insect cells [80] and mammalian cells expressing Cx40 [81].

Significantly, chemical/slow gating transitions between open and fully closed states and vice versa often display fluctuations (Figure 10C, red arrows). This suggests that the gate, likely to be CaM’s N-lobe, may flicker in and out of the channel’s mouth before settling.

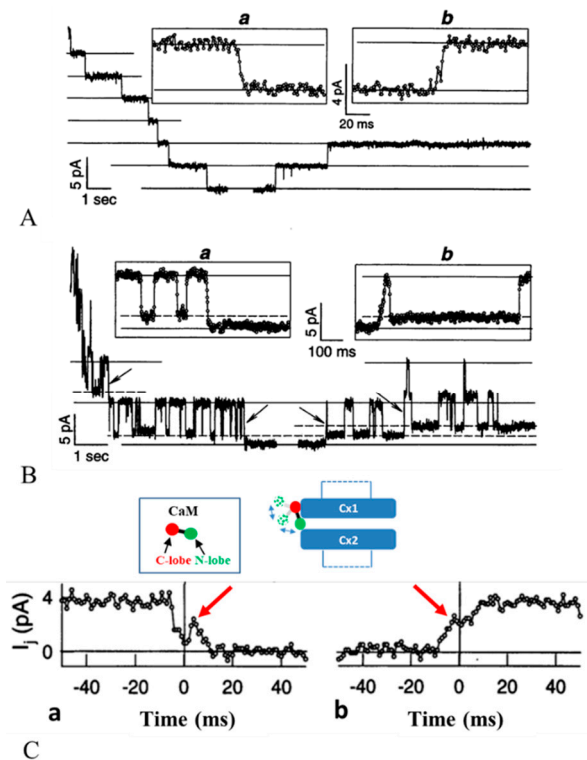


**Figure 10.** Effects of 100% CO<sub>2</sub> on single-channel gating behavior in gap junctions of fibroblast pairs subjected to V<sub>j</sub> 30 (A) or 55 (B) mV. Gating was monitored before total uncoupling ((A,B) left traces) and at the initial recoupling phase ((A,B) right traces). With V<sub>j</sub> = 30 mV (A), each channel closes by a slow I<sub>j</sub> transition from open, y<sub>j</sub>(main state), to closed state ((A) left trace and inset (Aa)) and reopens with a slow transition from closed state to y<sub>j</sub>(main state)((A) right trace and inset (Ab)). With V<sub>j</sub> = 55 mV (B), the channels show two I<sub>j</sub> transition: (1) between open and closed state (120 pS, ~10 ms; (B) left trace, arrows and inset (Ba)), and (2) between open and residual state (90 pS, 2 ms; (B) left trace and inset (Bb)). The channels reopen by a slow I<sub>j</sub> transition to open state ((B) right trace, arrows and inset (Bb)), followed by fast flickering to residual state. Thus, the chemical gate closes slowly and completely, while the fast V<sub>j</sub> gate closes fast and partially. Chemical gate transitions between open and fully closed states (Ca) and vice versa (Cb), often display fluctuations (C, red arrows), suggesting that the gate (CaM's N-lobe?) may flicker in and out of the channel's mouth before settling (C, inset). From [79].

Later studies provided further evidence for V<sub>j</sub> sensitivity of the chemical/slow gate [37,53,77,82] and for a CaM role in its behavior [37,38]. These findings confirm evidence that the chemical/slow gate behaves like a slow V<sub>j</sub>-sensitive gate. In the absence of uncouplers, chemical/slow gating activity is seldom observed. An exception are Cx45 channels, several of which are closed by the chemical/slow gate even at resting [Ca<sup>2+</sup>]<sub>i</sub> and pH<sub>i</sub> [38,74]. In addition to Cx45 channels, the chemical/slow gate is occasionally active in various channels made of connexin mutants (see in the following) and is activated in wild-type Cx32 channels by large V<sub>j</sub> gradients [82] (see in the following).

### 3.3. The Chemical/Slow Gate of Cx32 Channels Closes with V<sub>j</sub> Gradients

It has been generally thought that the chemical/slow gate is mostly inactive in the absence of uncouplers or connexin mutations. In contrast, in 2007 we reported that this gate can be activated by applying series of large V<sub>j</sub> gradients (Figure 11) [82]. In channels expressing Cx32 wild-type (Figure 11A) or the mutant Cx32-D225 (CT-truncated at res. 225; Figure 11B), the application of series of -100 mV V<sub>j</sub> pulses induces peak (I<sub>j</sub>PK) and steady-state (I<sub>j</sub>SS) I<sub>j</sub> to gradually drop (Figure 11A,B) [82]. G<sub>j</sub> steady state (G<sub>j</sub>SS) drops less dramatically than G<sub>j</sub> peak (G<sub>j</sub>PK), so that the ratio G<sub>j</sub>SS/G<sub>j</sub>PK progressively increases (Figure 11D). G<sub>j</sub> peak drops exponentially with the first 6–7 V<sub>j</sub> pulses by 50–60%, eventually reaching a steady state (Figure 11C). Most likely, while the first 6–7 pulses activate both chemical/slow

gate and fast Vj gate, the following pulses only activate the fast Vj gate of the remaining open channels (Figure 11A,B). Gj, monitored during recovery by applying small Vj pulses, slowly recovers, often achieving values greater than initial ones. Greater effects were obtained with the mutant Cx32-D225 [82] (Figure 11B–D), indicating that this degree of CT deletion does not eliminate the efficiency of the chemical/slow gate, but rather renders it more Vj-sensitive.

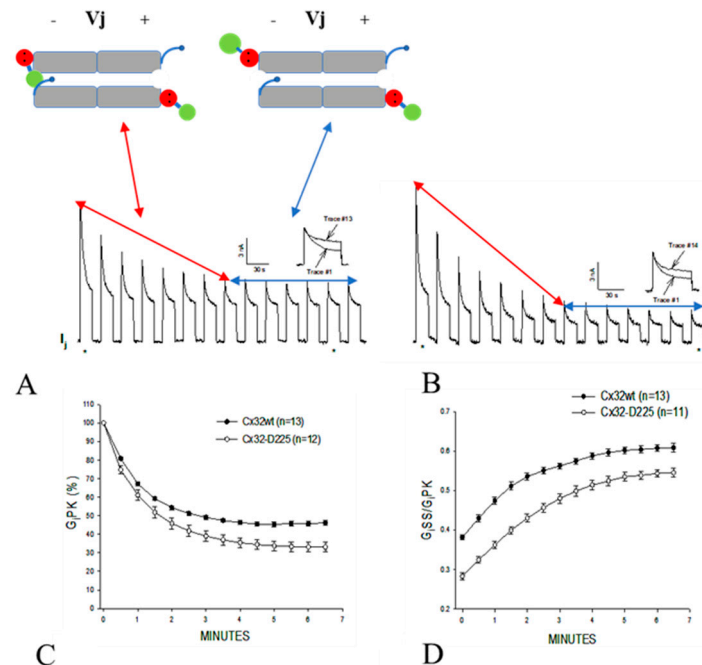


**Figure 11.** Slow Gj decay in oocytes expressing either Cx32 or its CT-truncated mutant (Cx32-D225) subjected to long  $-100$  mV Vj pulses. (A,B) show junctional current (Ij) tracings recorded from Cx32wt and Cx32-D225, respectively. Note the gradual drop in Ij-Peak (IjPK) and, to a lesser extent, Ij-Steady-State (IjSS; A and B). GjPK drops exponentially by 50–60%, eventually reaching steady state (C). GjSS/GjPK increases by 60% and 93% in Cx32wt and Cx32-D225, respectively (D). The large drop in Ij during the first 8 pulses is likely to result from the closure of both chemical/slow gate and fast Vj gate ((A,B) double-headed red arrows and left drawing). The Ij behavior of the following 6 Vj pulses is likely to reflect the closure of only the fast Vj gate of the remaining open channels ((A,B) double-headed blue arrows and right drawing). From [82].

With Vj polarity reversal, GjPK and GjSS increase slightly before dropping, as compared to the last few pulses of the previous series, (Figure 12A,B). Since both fast Vj gate and chemical/slow gate of Cx32 channels close at the negative side of Vj with Vj polarity reversal, previously the closed hemichannel gates, now at positive Vj side, start opening, while those at the negative Vj side start closing. If opening and closing kinetics were identical, GjPK and GjSS would not change from the last pulse of the series and the first pulse of the new series. However, since GjPK and GjSS are higher following Vj polarity reversal it is likely that Vj positive is more efficient and faster at opening hemichannel than Vj negative at closing them. Based on our hypothesis that the chemical/slow gate is the N-lobe of CaM, these data would suggest that the N-lobe's displacement by positive Vj from the channels' mouth is more rapid than its insertion into the mouth by negative Vj. Since this phenomenon is more pronounced with Cx32-D225 channels (Figure 12A,B) it is possible that the absence of the CT domain facilitates the displacement of the CaM's N-lobe away from the channel's mouth. The CT deletion may also facilitate channel plugging by the chemical gate, because the drop in IjPK and GjPK is much greater with Cx32-D225 than Cx32 wild-type channels (Figure 11A–C and Figure 12B).

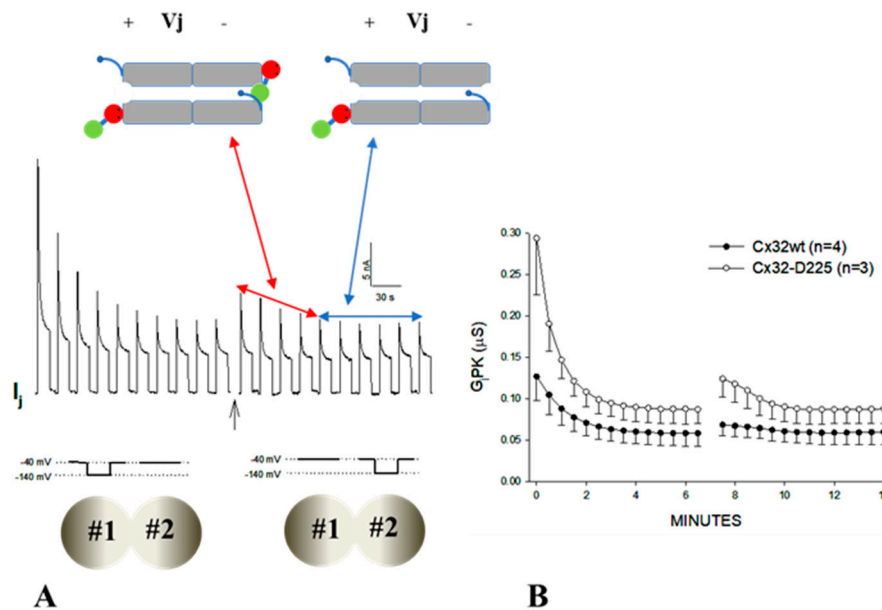


**Figure 12.** Effect of Vj polarity-reversal on junctional conductance ( $G_j$ ) in oocyte pairs expressing either Cx32 subjected to Vj pulses of  $-100$  mV. The  $I_j$  and  $G_j$ PK records ((A,B) respectively) show that in the first few pulses of the second series peak  $I_j$  ( $I_j$ PK; A, arrow) and consequently  $G_j$ PK (B) are substantially greater than that of the last pulse of the first series. This indicates that positive Vj is more effective in opening hemichannels than negative Vj in closing them. Significantly, this phenomenon is more pronounced with Cx32-D225 channels (B). From [82].

These data clearly indicate that the gate responsible for the exponential  $G_j$  drop is the chemical/slow gate, and not the fast Vj-gate. The presence of chemical/slow gating activity in Cx32's wild-type channels indicates that this gate (CaM's N-lobe?) can be made operational by large Vj gradients even in the absence of uncouplers and/or mutations. In fact, these data [82] confirm earlier evidence of Vj-induced slow-gating events to zero channel conductance in Cx32-expressing cells [83]. The behaviors previously described confirm the direct role of CaM in chemical/slow gating (CaM-Cork mechanism) because they are all strongly reduced by the inhibition of CaM expression [1,37,38].

#### 4. Calmodulin Cork Model—One Molecule, Two Mechanisms

Based on data described previously, we have proposed two mechanisms for the CaM-driven gating model. In one, "Ca-CaM-Cork", gating is initiated by  $Ca^{2+}$ -induced activation of the CaM's N-lobe (Figure 13D). In the other, "CaM-Cork", gating occurs without a  $[Ca^{2+}]_i$  rise above resting values. Ca-CaM-Cork gating is only reversed by a return of  $[Ca^{2+}]_i$  to resting values, while CaM-Cork gating is reversed by Vj positive at the gated side.

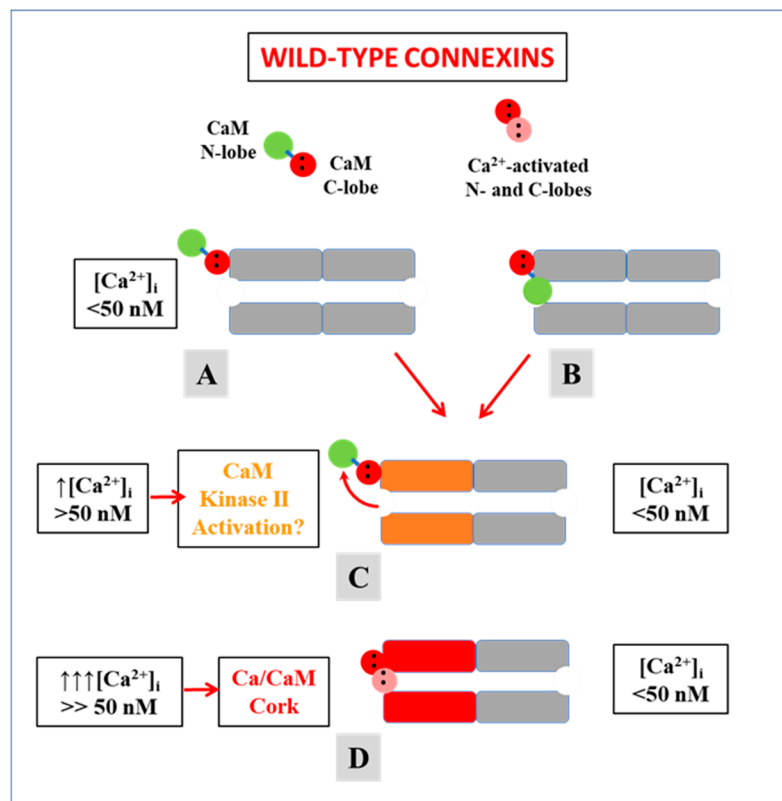


**Figure 13.** Schematic representation of Ca-CaM-Cork gating. Our hypothesis is that under normal conditions, while most channels are open (A) some are closed (B) by the CaM-Cork mechanism (B). With a small  $[Ca^{2+}]_i$  rise above resting values, CaMKII becomes activated, possibly resulting in the opening of CaM-Cork gated channels (C; orange connexins). With greater  $[Ca^{2+}]_i$  rise the  $Ca^{2+}$ -activated CaM's N-lobe interacts hydrophobically and electrostatically with the connexin's gating site and plugs the channel's pore (D; red connexins), probably also causing conformational changes in connexins (D).

#### 4.1. Ca-CaM-Cork Gating

There is evidence that in most coupled cells, especially in those expressing Cx45, a number of channels are in closed state even at resting  $[Ca^{2+}]_i$  [38,74] (Figure 13A,B) [38,84]. We believe that some channels in closed state at rest (Figure 13B) might be gated by the CaM-Cork mechanism (see in the following). Our hypothesis is that with a small  $[Ca^{2+}]_i$  rise above resting values the CaMKII cascade is likely to be activated, resulting in the opening of CaM-Cork gated channels (Figure 13C)—see initial G<sub>j</sub> rise in Figures 2 and 3. In contrast, greater  $[Ca^{2+}]_i$  rise would activate the CaM's N-lobe, enabling it to bind to a CaM's connexin site and plug the channel's mouth (Figure 13D) [1,4,53]. At resting  $[Ca^{2+}]_i$ , CaM is believed to be linked to each connexin by the C-lobe, probably at the CL2 site (Figure 5) [55,56], while the N-lobe in most channels is likely to be free. In Cx32 channels, the CaM's lobe may be unable to access the channel's mouth by the postulated CL1-CT1 interaction (Figure 14) [1,64].

The C-lobe's  $Ca^{2+}$ -affinity constant is greater than that of the N-lobe by almost one order of magnitude [41,85]. Thus, it is likely that the N-lobe only interacts with the connexin's gating site (CL2 or NT) with  $[Ca^{2+}]_i$  rises above resting levels. This model agrees with evidence for independent functions of N- and C-lobes in the interaction with Cx32 [59].

With a  $[Ca^{2+}]_i$  rise, one possibility is that in all of the six CaMs anchored to the connexon the N-lobes are activated, bind to the NT or CL2 sites of the same connexin and change connexins conformation. The conformational change would allow one of the six N-lobes to access the channel's mouth and plug the pore by binding to the NT or CL2 site of the opposite connexin hydrophobically and electrostatically. Another possibility is that while all of the N-lobes are activated one wins the

competition (first comes first served), binds to a site (NT or CL2) of the opposite connexin and plugs the pore by interacting with the site hydrophobically and electrostatically.

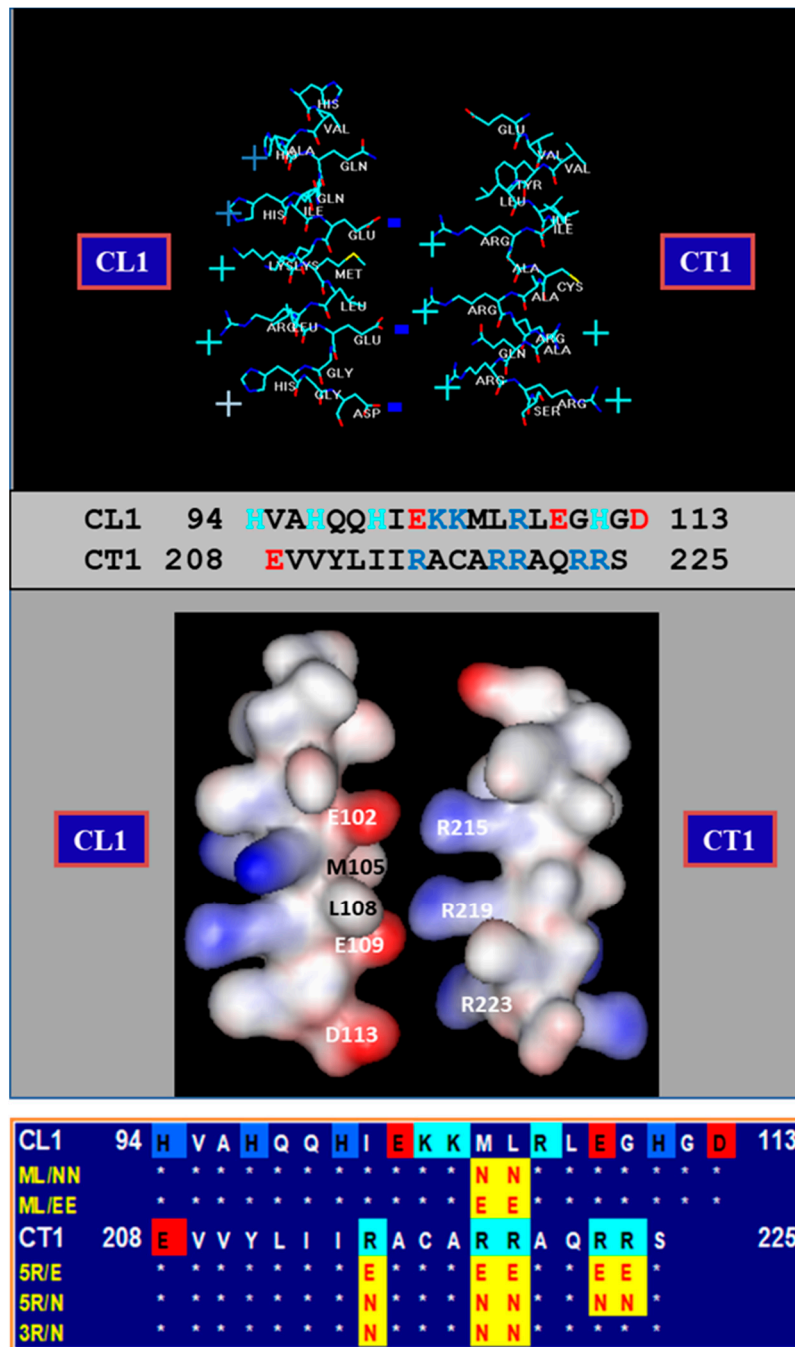


**Figure 14.** Cx32's CL1 (first half of CL) and CT1 (initial domain of CT) domains in  $\alpha$ -helical conformation. Our hypothesis is that in coupled conditions CL1 and CT1 interact electrostatically (negative CL1, positive CT1) and hydrophobically. CL1 and CT1 mutation (bottom panel) are believed to prevent the interaction allowing the negatively charged CaM's N-lobe to access the positively charged channel's mouth and plugging it by interaction with it electrostatically (CaM-Cork model). We suggest that with an increase in  $[Ca^{2+}]_i$  the activated CaM's N-lobe accesses the gating site and plugs the channel's mouth by breaking the CL1-CT1 interaction (Ca-CaM-Cork model).

#### 4.2. CaM-Cork Gating

The CaM-Cork mechanism is demonstrated by the behavior of heterotypic mutant-Cx32 channels (Figure 15A) [37,77], homotypic Cx45 channels and Cx32 channels subjected to large  $V_j$  gradients negative at the gating site (Figure 15B) [82]. Our hypothesis is that at the mutant side of mutant-Cx32 and mutant-Cx26 channels (see previously) a CaM's N-lobe can access the channel's mouth even at resting  $[Ca^{2+}]_i$  (Figure 15Aa)—perhaps, the mutations make the channel's mouth unprotected. The N-lobe would interact only electrostatically with the channel's mouth, such that  $V_j$  positive at the mutant hemichannel's side could release it from the mouth (Figure 15Ab) [1,37,77]. Significantly, both the negatively charged CaM lobes and the positively charged channel's mouth are  $\sim 35$  Å in size (Figure 16A–C).

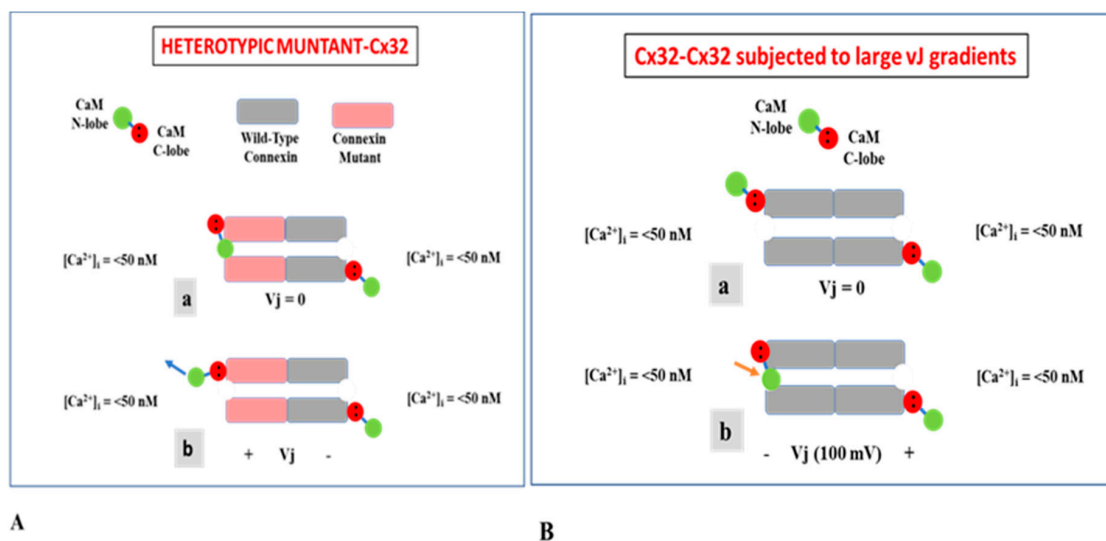


**Figure 15.** Schematic representation of CaM-Cork gating. CaM is anchored to connexins by its C-lobe at resting  $[Ca^{2+}]_i$  (A,B). Certain connexin mutations enable the negatively charged CaM's N-lobe to access the channel's pore and plug it by interacting electrostatically with the positively charged channel's mouth even at resting  $[Ca^{2+}]_i$  (Aa); the N-lobe can be moved out of the pore with  $V_j$  gradients positive at the mutant side (Ab). In wild-type connexins (Cx32-CX32), with the application of large  $V_j$  gradients the N-lobe can be reversibly forced to plug the channel's mouth at the negative side of  $V_j$  at resting  $[Ca^{2+}]_i$  (Bb).

As previously pointed out, the behavior of CaM-Cork gating is a manifestation of the chemical-slow gate (CaM's N-lobe?) rather than that of the fast  $V_j$ -gate because  $V_j$  positive at mutant side opens channels of both "negative" (Cx32) and positive (Cx26) fast  $V_j$ -gaters (Figure 9) [1,4]. If the fast  $V_j$ -gates were involved,  $V_j$  positive at the mutant side would close, not open mutant-Cx26 channels (4pos/E-26).

Cytoplasmic domains of connexins have a high basic/acidic amino acid ratio. In Cx32, for example, neglecting most of CT whose deletion by 84% has no effect on gating sensitivity [63,64], and assigning values of one for R, K, D and E and 1/2 for H, one counts 18 basic and six acidic residues per connexin—108 and 36, respectively, per connexon. In view of the effectiveness of short-range electric fields, the  $V_j$ -sensitive slow-gating behavior of mutant Cx32 channels would be expected to manifest itself only if the gating CaM lobe were near the channel's mouth.

Why would the channel's mouth be accessible to the CaM's N-lobe only in Cx32 mutants? Perhaps, in Cx32 and other connexins, the channel's mouth is not very accessible due to the postulated CL1-CT1 electrostatic/hydrophobic interaction (Figure 14) [1,37,64,77,86]. The potential absence of this interaction in mutant channels lacking CT1's positive charges (Figure 14; 5R/N, 5R/T and 3R/N), in mutant channels in which charges are converted to negative (Figure 14; 5R/E) [64,77,86], and in mutant channels in which the hydrophobic CL1's amino acids M105 and L106 are mutated to N or E

(Figure 13; ML/NN, ML/EE, ML/NN + 3R/N) [37], would be expected to enable the N-lobe to access the channel's mouth. In tandem-Cx32 channels, the NT-CT linkage in tandem might prevent the proposed CL1-CT1 interaction [37,77].

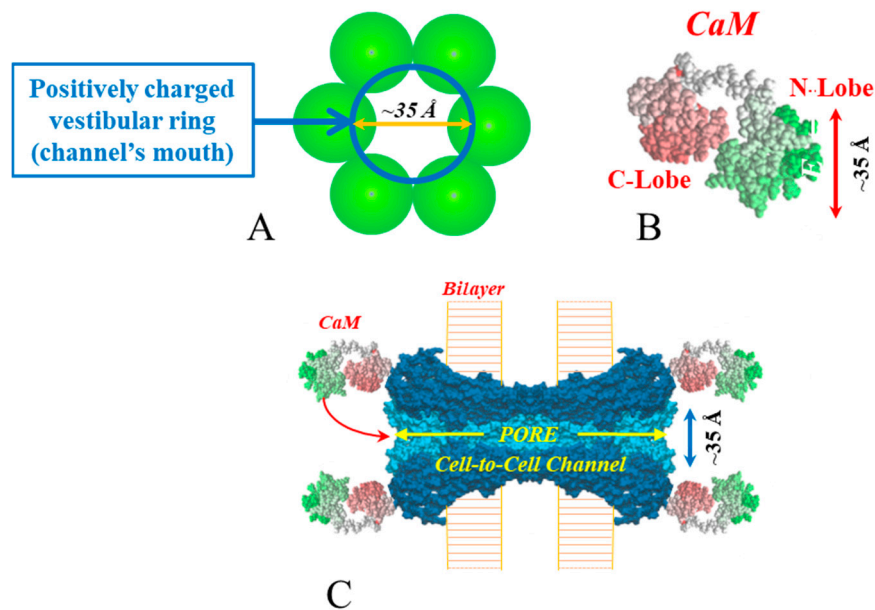


**Figure 16.** Both the positively charged channel's mouth (A,C) and the negatively charged CaM lobes (B) are  $\sim 25 \times 35 \text{ \AA}$  in size. Therefore, a CaM lobe could interact and fit well within the positively charged connexon's mouth (vestibule) (A,C). In (C) the channel is split lengthwise so that the pore diameter (light blue area) is seen throughout the entire channel's length. Both the CaM and connexon images (B,C) were provided by Drs. Francesco Zonta and Mario Bortolozzi (VIMM, University of Padua, Italy).

Based on evidence for the effect on G<sub>j</sub> of large V<sub>j</sub> gradients applied to Cx32 channels (Figures 10 and 11) [82], it seems possible that the gating element (CaM's N-lobe?) could be forced to plug the mouth of the hemichannel subjected to negative V<sub>j</sub> in the absence of connexin mutations or Ca<sup>2+</sup>-activation. Thus, the hemichannel's mouth might not be completely inaccessible [82].

In some channels made of wild-type connexins, V<sub>j</sub> gradients may not be needed for forcing the gating particle (CaM's N-lobe?) into the channel's mouth. In fact, in Cx45-expressing cells, for example, many channels are closed by the chemical/slow gate at V<sub>j</sub> = 0 and resting [Ca<sup>2+</sup>]<sub>i</sub> [38,74]. In these cases, the closed channels are likely to be gated by the CaM-Cork mechanism and are likely to be opened by small increases in [Ca<sup>2+</sup>]<sub>i</sub> possibly via activation of the CaMKII cascade. Perhaps, the postulated CL1-CT1 interaction is weaker in Cx45 channels. Since inhibition of CaM expression inhibits the chemical gating of Cx45 channels [38], the gating element is likely to be a CaM lobe electrostatically bound to the channel's pore.

## 5. Conclusion

Evidence that gap junction mediated cell communication is finely regulated by nanomolar [Ca<sup>2+</sup>]<sub>i</sub> via the direct action of Ca<sup>2+</sup>-CaM indicates that gap junction channel gating is not just a safety mechanism for protecting cells from damaged/dead neighbors (healing-over). Rather, it is also a mechanism designed to finely modulate cell-cell exchange of small molecules.

We have proposed a two-facet CaM-mediated gating mechanism: Ca-CaM-Cork and CaM-Cork. In summary:

1. At resting [Ca<sup>2+</sup>]<sub>i</sub>, (<50nM) some channels are spontaneously closed by the CaM-Cork gating mechanism.

2. With moderate  $[Ca^{2+}]_i$  rise (50–100 nM, the CaMKII cascade may be activated causing channels closed by the CaM-Cork mechanism to open.
3. With greater  $[Ca^{2+}]_i$  rise (>100 nM), the channels start closing by the Ca-CaM-Cork mechanism. CaM lobe channel mouth plugging is likely to include connexin conformational changes.
4. CaM-Cork gated channels could be reopened by Vj positive at gated side, but since they would close at the negative side no Gj change would occur. This is not the case with heterotypic channels between wild-type connexins paired with more gating-sensitive mutants.
5. Most Ca-CaM-Cork gated channels reopen with a drop in  $[Ca^{2+}]_i$  to resting values (<50 nM). However, with prolonged exposure to high  $[Ca^{2+}]_i$ , channel gating may not be reversible.

Many questions still need to be answered in terms of molecular details, such as: Is CaM anchored to the NT or the CL2 domain? Is CaM anchored to connexins by the C-lobe or the N-lobe? Is the gating lobe the N-lobe or the C-lobe? Does the gating lobe bind to the CL2 or the NT CaM binding site? Are all of the CaMs anchored to a connexon  $Ca^{2+}$ -activated? If so, how many lobes gate the channel? Does CaM activation cause connexin conformational changes?

**Funding:** This research received no external funding.

**Conflicts of Interest:** The authors declare no conflict of interest.

## References

1. Peracchia, C. *Gap Junction Structure and Chemical Regulation: Direct Calmodulin Role in Cell-to-Cell Channel Gating*; Elsevier: London, UK, 2019.
2. Harris, A.L.; Locke, D. *Connexins—A Guide*; Humana Press/Springer: New York, NY, USA, 2009.
3. Evans, W.H. Cell communication across gap junctions: A historical perspective and current developments. *Biochem. Soc. Trans.* **2015**, *43*, 450–459. [[CrossRef](#)] [[PubMed](#)]
4. Peracchia, C.; Wang, X.C.; Peracchia, L.L. Behavior of Chemical and Slow Voltage-Gates of Connexin Channels. The cork Gating Hypothesis. In *Gap Junctions—Molecular Basis of Cell Communication in Health and Disease*; Peracchia, C., Ed.; Academic Press: San Diego, CA, USA, 2000; pp. 271–295.
5. Noma, A.; Tsuboi, N. Dependence of junctional conductance on proton, calcium and magnesium ions in cardiac paired cells of guinea-pig. *J. Physiol.* **1987**, *382*, 193–211. [[CrossRef](#)] [[PubMed](#)]
6. Noma, A.; Tsuboi, N. Direct measurement of the gap junctional conductance under the influence of  $Ca^{2+}$  in dissociated paired myocytes of guinea-pig. *Jpn. Heart J.* **1986**, *27*, 161–166. [[PubMed](#)]
7. Dekker, L.R.; Fiolet, J.W.; VanBavel, E.; Coronel, R.; Opthof, T.; Spaan, J.A.; Janse, M.J. Intracellular  $Ca^{2+}$ , intercellular electrical coupling, and mechanical activity in ischemic rabbit papillary muscle. Effects of preconditioning and metabolic blockade. *Circ. Res.* **1996**, *79*, 237–246.
8. Peracchia, C. Effects of caffeine and ryanodine on low  $pH_i$ -induced changes in gap junction conductance and calcium concentration in crayfish septate axons. *J. Membr. Biol.* **1990**, *117*, 79–89. [[CrossRef](#)]
9. Peracchia, C. Increase in gap junction resistance with acidification in crayfish septate axons is closely related to changes in intracellular calcium but not hydrogen ion concentration. *J. Membr. Biol.* **1990**, *113*, 75–92. [[CrossRef](#)]
10. Peracchia, C.; Wang, X.; Li, L.; Peracchia, L.L. Inhibition of calmodulin expression prevents low-pH-induced gap junction uncoupling in *Xenopus* oocytes. *Pflüg. Arch.* **1996**, *431*, 379–387. [[CrossRef](#)]
11. Neyton, J.; Trautmann, A. Single-channel currents of an intercellular junction. *Nature* **1985**, *317*, 331–335. [[CrossRef](#)]
12. Lazrak, A.; Peracchia, C. Gap junction gating sensitivity to physiological internal calcium regardless of pH in Novikoff hepatoma cells. *Biophys. J.* **1993**, *65*, 2002–2012. [[CrossRef](#)]
13. Lazrak, A.; Peres, A.; Giovannardi, S.; Peracchia, C. Ca-mediated and independent effects of arachidonic acid on gap junctions and Ca-independent effects of oleic acid and halothane. *Biophys. J.* **1994**, *67*, 1052–1059. [[CrossRef](#)]
14. Enkvist, M.O.; McCarthy, K.D. Astroglial gap junction communication is increased by treatment with either glutamate or high  $K^+$  concentration. *J. Neurochem.* **1994**, *62*, 489–495. [[CrossRef](#)] [[PubMed](#)]

15. Giaume, C.; Venance, L. Characterization and regulation of gap junction channels in cultured astrocytes. In *Gap Junctions in the Nervous System*; Spray, D.C., Dermietzel, R., Eds.; R.G Landes Medical Pub.: Austin, TX, USA, 1996; pp. 135–157.
16. Cotrina, M.L.; Kang, J.; Lin, J.H.; Bueno, E.; Hansen, T.W.; He, L.; Liu, Y.; Nedergaard, M. Astrocytic gap junctions remain open during ischemic conditions. *J. Neurosci.* **1998**, *18*, 2520–2537. [[CrossRef](#)]
17. Crow, J.M.; Atkinson, M.M.; Johnson, R.G. Micromolar levels of intracellular calcium reduce gap junctional permeability in lens cultures. *Investig. Ophthalmol. Vis. Sci.* **1994**, *35*, 3332–3341.
18. Dakin, K.; Zhao, Y.; Li, W.H. LAMP, a new imaging assay of gap junctional communication unveils that Ca<sup>2+</sup> influx inhibits cell coupling. *Nat. Methods* **2005**, *2*, 55–62. [[CrossRef](#)]
19. Xu, Q.; Kopp, R.F.; Chen, Y.; Yang, J.J.; Roe, M.W.; Veenstra, R.D. Gating of connexin 43 gap junctions by a cytoplasmic loop calmodulin binding domain. *Am. J. Physiol. Cell Physiol.* **2012**, *302*, C1548–C1556. [[CrossRef](#)] [[PubMed](#)]
20. Matthews, E.K.; Petersen, O.H. Pancreatic acinar cells: Ionic dependence of the membrane potential and acetylcholine-induced depolarization. *J. Physiol.* **1973**, *231*, 283–295. [[CrossRef](#)] [[PubMed](#)]
21. Scheele, G.A.; Palade, G.E. Studies on the guinea pig pancreas. Parallel discharge of exocrine enzyme activities. *J. Biol. Chem.* **1975**, *250*, 2660–2670. [[PubMed](#)]
22. Iwatsuki, N.; Petersen, O.H. Membrane potential, resistance, and intercellular communication in the lacrimal gland: Effects of acetylcholine and adrenaline. *J. Physiol.* **1978**, *275*, 507–520. [[CrossRef](#)] [[PubMed](#)]
23. Iwatsuki, N.; Petersen, O.H. Pancreatic acinar cells: Acetylcholine-evoked electrical uncoupling and its ionic dependency. *J. Physiol.* **1978**, *274*, 81–106. [[CrossRef](#)]
24. Iwatsuki, N.; Petersen, O.H. Electrical coupling and uncoupling of exocrine acinar cells. *J. Cell Biol.* **1978**, *79*, 533–545. [[CrossRef](#)]
25. Mears, D.; Sheppard, N.F., Jr.; Atwater, I.; Rojas, E. Magnitude and modulation of pancreatic beta-cell gap junction electrical conductance in situ. *J. Membr. Biol.* **1995**, *146*, 163–176. [[CrossRef](#)] [[PubMed](#)]
26. Spray, D.C.; Harris, A.L.; Bennett, M.V. Gap junctional conductance is a simple and sensitive function of intracellular pH. *Science* **1981**, *211*, 712–715. [[CrossRef](#)] [[PubMed](#)]
27. Peracchia, C. Possible involvement of caffeine- and rianodine-sensitive calcium stores in low pH-induced regulation of gap junction channels. In *Biophysics of Gap Junction Channels*; Peracchia, C., Ed.; CRS Press: Boca Raton, FL, USA, 1990; pp. 13–28.
28. Peracchia, C. Calmodulin-mediated regulation of gap junction channels. *Int. J. Mol. Sci.* **2020**, *21*, 485. [[CrossRef](#)] [[PubMed](#)]
29. Peracchia, C. Communicating junctions and calmodulin: Inhibition of electrical uncoupling in *Xenopus* embryo by calmidazolium. *J. Membr. Biol.* **1984**, *81*, 49–58. [[CrossRef](#)]
30. Peracchia, C.; Bernardini, G.; Peracchia, L.L. Is calmodulin involved in the regulation of gap junction permeability? *Pflüg. Arch.* **1983**, *399*, 152–154. [[CrossRef](#)]
31. Peracchia, C.; Bernardini, G.; Peracchia, L.L. A calmodulin inhibitor prevents gap junction crystallization and electrical uncoupling. *J. Cell Biol.* **1981**, *91*, 124a.
32. Lurtz, M.M.; Louis, C.F. Calmodulin and protein kinase C regulate gap junctional coupling in lens epithelial cells. *Am. J. Physiol. Cell Physiol.* **2003**, *285*, C1475–C1482. [[CrossRef](#)]
33. Peracchia, C. Calmodulin-like proteins and communicating junctions. Electrical uncoupling of crayfish septate axons is inhibited by the calmodulin inhibitor W7 and is not affected by cyclic nucleotides. *Pflüg. Arch.* **1987**, *408*, 379–385. [[CrossRef](#)]
34. Wojtczak, J.A. Electrical uncoupling induced by general anesthetics: A calcium-independent process? In *Gap Junctions*; Bennett, M.V.L., Spray, D.C., Eds.; Cold Spring Harbor Laboratory: Cold Spring Harbor, NY, USA, 1985; pp. 167–175.
35. Tuganowski, W.; Korczynska, I.; Wasik, K.; Piatek, G. Effects of calmidazolium and dibutyryl cyclic AMP on the longitudinal internal resistance in sinus node strips. *Pflüg. Arch.* **1989**, *414*, 351–353. [[CrossRef](#)]
36. Gandolfi, S.A.; Duncan, G.; Tomlinson, J.; Maraini, G. Mammalian lens inter-fiber resistance is modulated by calcium and calmodulin. *Curr. Eye Res.* **1990**, *9*, 533–541. [[CrossRef](#)]
37. Peracchia, C.; Wang, X.G.; Peracchia, L.L. Slow gating of gap junction channels and calmodulin. *J. Membr. Biol.* **2000**, *178*, 55–70. [[CrossRef](#)]
38. Peracchia, C.; Young, K.C.; Wang, X.G.; Peracchia, L.L. Is the voltage gate of connexins CO<sub>2</sub>-sensitive? *Cx45 channels and inhibition of calmodulin expression*. *J. Membr. Biol.* **2003**, *195*, 53–62. [[PubMed](#)]

39. Peracchia, C.; Sotkis, A.; Wang, X.G.; Peracchia, L.L.; Persechini, A. Calmodulin directly gates gap junction channels. *J. Biol. Chem.* **2000**, *275*, 26220–26224. [[CrossRef](#)] [[PubMed](#)]
40. Sotkis, A.; Wang, X.G.; Yasumura, T.; Peracchia, L.L.; Persechini, A.; Rash, J.E.; Peracchia, C. Calmodulin colocalizes with connexins and plays a direct role in gap junction channel gating. *Cell Commun. Adhes.* **2001**, *8*, 277–281. [[CrossRef](#)] [[PubMed](#)]
41. Persechini, A.; Gansz, K.J.; Paresi, R.J. Activation of myosin light chain kinase and nitric oxide synthase activities by engineered calmodulins with duplicated or exchanged EF hand pairs. *Biochemistry* **1996**, *35*, 224–228. [[CrossRef](#)]
42. Morley, G.E.; Taffet, S.M.; Delmar, M. Intramolecular interactions mediate pH regulation of connexin43 channels. *Biophys. J.* **1996**, *70*, 1294–1302. [[CrossRef](#)]
43. Delmar, M.; Stergiopoulos, K.; Homma, N.; Ek-Vitorin, J.F.; Taffet, S.M. A ball-and-chain model for chemical regulation of connexin 43. In *Gap Junctions*; Werner, R., Ed.; IOS Press: Amsterdam, The Netherlands, 1998; pp. 8–12.
44. Delmar, M.; Stergiopoulos, K.; Homma, N.; Calero, G.; Morley, G.; Ek-Vitorin, J.F.; Taffet, S.M. A molecular model for the chemical regulation of the connexin43 channels: The “ball-and-chain” hypothesis. In *Gap Junctions. Molecular Basis of Cell Communication in Health and Disease*; Peracchia, C., Ed.; Academic Press: San Diego, CA, USA, 2000; pp. 223–248.
45. Wei, S.; Cassara, C.; Lin, X.; Veenstra, R.D. Calcium-calmodulin gating of a pH-insensitive isoform of connexin43 gap junctions. *Biochem. J.* **2019**, *476*, 1137–1148. [[CrossRef](#)]
46. Pereda, A.E.; Bell, T.D.; Chang, B.H.; Czernik, A.J.; Nairn, A.C.; Soderling, T.R.; Faber, D.S. Ca<sup>2+</sup>/calmodulin-dependent kinase II mediates simultaneous enhancement of gap-junctional conductance and glutamatergic transmission. *Proc. Natl. Acad. Sci. USA* **1998**, *95*, 13272–13277. [[CrossRef](#)]
47. De Pina-Benabou, M.H.; Srinivas, M.; Spray, D.C.; Scemes, E. Calmodulin kinase pathway mediates the K<sup>+</sup>-induced increase in Gap junctional communication between mouse spinal cord astrocytes. *J. Neurosci.* **2001**, *21*, 6635–6643. [[CrossRef](#)]
48. De Vuyst, E.; Wang, N.; Decrock, E.; De, B.M.; Vinken, M.; Van, M.M.; Lai, C.; Culot, M.; Rogiers, V.; Cecchelli, R.; et al. Ca<sup>2+</sup> regulation of connexin 43 hemichannels in C6 glioma and glial cells. *Cell Calcium* **2009**, *46*, 176–187. [[CrossRef](#)]
49. Huang, R.Y.; Laing, J.G.; Kanter, E.M.; Berthoud, V.M.; Bao, M.; Rohrs, H.W.; Townsend, R.R.; Yamada, K.A. Identification of CaMKII phosphorylation sites in Connexin43 by high-resolution mass spectrometry. *J. Proteome Res.* **2011**, *10*, 1098–1109. [[CrossRef](#)] [[PubMed](#)]
50. Zhang, X.; Qi, Y. Role of intramolecular interaction in connexin50: Mediating the Ca<sup>2+</sup>-dependent binding of calmodulin to gap junction. *Arch. Biochem. Biophys.* **2005**, *440*, 111–117. [[CrossRef](#)] [[PubMed](#)]
51. Zhang, X.; Zou, T.; Liu, Y.; Qi, Y. The gating effect of calmodulin and calcium on the connexin50 hemichannel. *Biol. Chem.* **2006**, *387*, 595–601. [[CrossRef](#)] [[PubMed](#)]
52. Siu, R.C.; Smirnova, E.; Brown, C.A.; Zoidl, C.; Spray, D.C.; Donaldson, L.W.; Zoidl, G. Structural and Functional Consequences of Connexin 36 (Cx36) Interaction with Calmodulin. *Front. Mol. Neurosci.* **2016**, *9*, 120. [[CrossRef](#)]
53. Peracchia, C. Chemical gating of gap junction channels; roles of calcium, pH and calmodulin. *Biochim. Biophys. Acta* **2004**, *1662*, 61–80. [[CrossRef](#)]
54. Zou, J.; Salarian, M.; Chen, Y.; Zhuo, Y.; Brown, N.E.; Hepler, J.R.; Yang, J. Direct Visualization of Interaction between Calmodulin and Connexin45. *Biochem. J.* **2017**, *474*, 4035–4051. [[CrossRef](#)]
55. Kerruth, S.; Coates, C.; Rezavi, S.A.; Peracchia, C.; Török, K. Calmodulin interaction with gap junction intracellular loop peptides. *Biophys. J.* **2018**, *114*, 468a. [[CrossRef](#)]
56. Kerruth, S.; Coates, C.; Rezavi, S.A.; Peracchia, C.; Török, K. Ca<sup>2+</sup>-dependent and -independent interaction of calmodulin with gap junction cytoplasmic loop peptides. *Biochem. J.* **2020**, submitted.
57. Peracchia, C. The calmodulin hypothesis for gap junction regulation six years later. In *Gap Junctions*; Hertzberg, E., Johnson, R.G., Alan, R., Eds.; Liss: New York, NY, USA, 1988; pp. 267–282.
58. Török, K.; Stauffer, K.; Evans, W.H. Connexin 32 of gap junctions contains two cytoplasmic calmodulin-binding domains. *Biochem. J.* **1997**, *326*, 479–483. [[CrossRef](#)]
59. Dodd, R.; Peracchia, C.; Stolady, D.; Török, K. Calmodulin association with connexin32-derived peptides suggests trans-domain interaction in chemical gating of gap junction channels. *J. Biol. Chem.* **2008**, *283*, 26911–26920. [[CrossRef](#)] [[PubMed](#)]

60. Stauch, K.; Kieken, F.; Sorgen, P. Characterization of the structure and intermolecular interactions between the connexin 32 carboxyl-terminal domain and the protein partners synapse-associated protein 97 and calmodulin. *J. Biol. Chem.* **2012**, *287*, 27771–27788. [[CrossRef](#)]
61. Sorgen, P.L.; Trease, A.J.; Spagnol, G.; Delmar, M.; Nielsen, M.S. Protein-protein interactions with connexin 43: Regulation and function. *Int. J. Mol. Sci.* **2018**, *19*, 1428. [[CrossRef](#)] [[PubMed](#)]
62. Burr, G.S.; Mitchell, C.K.; Keflemariam, Y.J.; Heidelberger, R.; O'Brien, J. Calcium-dependent binding of calmodulin to neuronal gap junction proteins. *Biochem. Biophys. Res. Commun.* **2005**, *335*, 1191–1198. [[CrossRef](#)]
63. Werner, R.; Levine, E.; Rabadan-Diehl, C.; Dahl, G. Gating properties of connexin32 cell-cell channels and their mutants expressed in *Xenopus* oocytes. *Proc. Biol. Sci.* **1991**, *243*, 5–11. [[PubMed](#)]
64. Wang, X.G.; Peracchia, C. Positive charges of the initial C-terminus domain of Cx32 inhibit gap junction gating sensitivity to CO<sub>2</sub>. *Biophys. J.* **1997**, *73*, 798–806. [[CrossRef](#)]
65. Wang, X.G.; Peracchia, C. Connexin 32/38 chimeras suggest a role for the second half of inner loop in gap junction gating by low pH. *Am. J. Physiol.* **1996**, *271*, C1743–C1749. [[CrossRef](#)] [[PubMed](#)]
66. Wang, X.; Li, L.; Peracchia, L.L.; Peracchia, C. Chimeric evidence for a role of the connexin cytoplasmic loop in gap junction channel gating. *Pflüg. Arch.* **1996**, *431*, 844–852. [[CrossRef](#)]
67. Zhou, Y.; Yang, W.; Lurtz, M.M.; Ye, Y.; Huang, Y.; Lee, H.W.; Chen, Y.; Louis, C.F.; Yang, J.J. Identification of the calmodulin binding domain of connexin 43. *J. Biol. Chem.* **2007**, *282*, 35005–35017. [[CrossRef](#)]
68. Chen, Y.; Zhou, Y.; Lin, X.; Wong, H.C.; Xu, Q.; Jiang, J.; Wang, S.; Lurtz, M.M.; Louis, C.F.; Veenstra, R.D.; et al. Molecular interaction and functional regulation of connexin50 gap junctions by calmodulin. *Biochem. J.* **2011**, *435*, 711–722. [[CrossRef](#)]
69. Zou, J.; Salarian, M.; Chen, Y.; Veenstra, R.; Louis, C.F.; Yang, J.J. Gap junction regulation by calmodulin. *FEBS Lett.* **2014**, *588*, 1430–1438. [[CrossRef](#)]
70. Zhou, Y.; Yang, W.; Lurtz, M.M.; Chen, Y.; Jiang, J.; Huang, Y.; Louis, C.F.; Yang, J.J. Calmodulin mediates the Ca<sup>2+</sup>-dependent regulation of Cx44 gap junctions. *Biophys. J.* **2009**, *96*, 2832–2848. [[CrossRef](#)] [[PubMed](#)]
71. Myllykoski, M.; Kuczera, K.; Kursula, P. Complex formation between calmodulin and a peptide from the intracellular loop of the gap junction protein connexin43: Molecular conformation and energetics of binding. *Biophys. Chem.* **2009**, *144*, 130–135. [[CrossRef](#)] [[PubMed](#)]
72. Peracchia, C.; Chen, J.T.; Peracchia, L.L. CO<sub>2</sub> sensitivity of voltage gating and gating polarity of gap junction channels—connexin40 and its COOH-terminus-truncated mutant. *J. Membr. Biol.* **2004**, *200*, 105–113. [[CrossRef](#)] [[PubMed](#)]
73. Yap, K.L.; Kim, J.; Truong, K.; Sherman, M.; Yuan, T.; Ikura, M. Calmodulin target database. *J. Struct. Funct. Genom.* **2000**, *1*, 8–14. [[CrossRef](#)]
74. Bukauskas, F.F.; Angele, A.B.; Verselis, V.K.; Bennett, M.V. Coupling asymmetry of heterotypic connexin 45/connexin 43-EGFP gap junctions: Properties of fast and slow gating mechanisms. *Proc. Natl. Acad. Sci. USA* **2002**, *99*, 7113–7118. [[CrossRef](#)]
75. Török, K.; Trentham, D.R. Mechanism of 2-chloro-(epsilon-amino-Lys75)-[6-[4-(N,N-diethylamino)phenyl]-1,3,5-triazin-4-yl]calmodulin interactions with smooth muscle myosin light chain kinase and derived peptides. *Biochemistry* **1994**, *33*, 12807–12820. [[CrossRef](#)] [[PubMed](#)]
76. Laird, D.W.; Puranam, K.L.; Revel, J.P. Turnover and phosphorylation dynamics of connexin43 gap junction protein in cultured cardiac myocytes. *Biochem. J.* **1991**, *273*, 67–72. [[CrossRef](#)] [[PubMed](#)]
77. Peracchia, C.; Wang, X.G.; Peracchia, L.L. Is the chemical gate of connexins voltage sensitive? Behavior of Cx32 wild-type and mutant channels. *Am. J. Physiol.* **1999**, *276*, C1361–C1373. [[PubMed](#)]
78. Verselis, V.K.; Ginter, C.S.; Bargiello, T.A. Opposite voltage gating polarities of two closely related connexins. *Nature* **1994**, *368*, 348–351. [[CrossRef](#)] [[PubMed](#)]
79. Bukauskas, F.F.; Peracchia, C. Two distinct gating mechanisms in gap junction channels: CO<sub>2</sub>-sensitive and voltage-sensitive. *Biophys. J.* **1997**, *72*, 2137–2142. [[CrossRef](#)]
80. Bukauskas, F.F.; Weingart, R. Voltage-dependent gating of single gap junction channels in an insect cell line. *Biophys. J.* **1994**, *67*, 613–625. [[CrossRef](#)]
81. Bukauskas, F.F.; Elfgang, C.; Willecke, K.; Weingart, R. Biophysical properties of gap junction channels formed by mouse connexin40 in induced pairs of transfected human HeLa cells. *Biophys. J.* **1995**, *68*, 2289–2298. [[CrossRef](#)]

82. Peracchia, C.; Salim, M.; Peracchia, L.L. Unusual slow gating of gap junction channels in oocytes expressing connexin32 or its COOH-terminus truncated mutant. *J. Membr. Biol.* **2007**, *215*, 161–168. [[CrossRef](#)] [[PubMed](#)]
83. Oh, S.; Ri, Y.; Bennett, M.V.; Trexler, E.B.; Verselis, V.K.; Bargiello, T.A. Changes in permeability caused by connexin 32 mutations underlie X-linked Charcot-Marie-Tooth disease. *Neuron* **1997**, *19*, 927–938. [[CrossRef](#)]
84. Bukauskas, F.F.; Jordan, K.; Bukauskiene, A.; Bennett, M.V.; Lampe, P.D.; Laird, D.W.; Verselis, V.K. Clustering of connexin 43-enhanced green fluorescent protein gap junction channels and functional coupling in living cells. *Proc. Natl. Acad. Sci. USA* **2000**, *97*, 2556–2561. [[CrossRef](#)]
85. Astegno, A.; La Verde, V.; Marino, V.; Dell’Orco, D.; Dominici, P. Biochemical and biophysical characterization of a plant calmodulin: Role of the N- and C-lobes in calcium binding, conformational change, and target interaction. *Biochim. Biophys. Acta* **2016**, *1864*, 297–307. [[CrossRef](#)] [[PubMed](#)]
86. Wang, X.G.; Peracchia, C. Molecular dissection of a basic COOH-terminal domain of Cx32 that inhibits gap junction gating sensitivity. *Am. J. Physiol.* **1998**, *275*, C1384–C1390. [[CrossRef](#)] [[PubMed](#)]



© 2020 by the author. Licensee MDPI, Basel, Switzerland. This article is an open access article distributed under the terms and conditions of the Creative Commons Attribution (CC BY) license (<http://creativecommons.org/licenses/by/4.0/>).